ACIBADEM MEHMET ALI AYDINLAR UNIVERSITY
INSTITUTE OF HEALTH SCIENCES

STABILITY ENHANCEMENT OF A NOVEL ANTIMICROBIAL PEPTIDE WITH THE COMBINATION OF DRUG DELIVERY SYSTEMS

SERAY ŞAHSUVAR
M.Sc. THESIS

DEPARTMENT OF MEDICAL BIOTECHNOLOGY

SUPERVISOR
Prof. Dr. Özge Can

SECONDARY SUPERVISOR
Assist. Prof. Dr. Özgül Gök

ISTANBUL-2023

ACIBADEM MEHMET ALI AYDINLAR UNIVERSITY
INSTITUTE OF HEALTH SCIENCES

STABILITY ENHANCEMENT OF A NOVEL ANTIMICROBIAL PEPTIDE WITH THE COMBINATION OF DRUG DELIVERY SYSTEMS

SERAY ŞAHSUVAR
M.Sc. THESIS

DEPARTMENT OF MEDICAL BIOTECHNOLOGY

SUPERVISOR
Prof. Dr. Özge Can

SECONDARY SUPERVISOR
Assist. Prof. Dr. Özgül Gök

ISTANBUL-2023

DECLARATION

I declare that this thesis work is my own work, I had no unethical behavior at any stages from the planning to the writing of the thesis, I obtained all the information in this thesis in accordance with academic and ethicel rules, I cited all the information and comments that were not obtained with this thesis work, and I provided resources in the list of references. I also declare that there was no violation of any patents and copyrights during the study and writing of this thesis.

29.04.2023

Seray Şahsuvar

PREFACE AND ACKNOWLEDGEMENT

Firstly, I would like to express my sincere gratitude to my advisor, Prof. Dr. Özge Can for his efforts, trust, and support for me. His mentoring and guidance throughout my master's degree has considerably support me in carrying out this research. I also would like to thank to my co-supervisor Assist. Prof. Özgül Gök for her support, patient and always motivating me. I am grateful to both of my mentors for shedding light on my path, and always pushing me further.

I am grateful to GOK Lab members as a second family who constantly encourage and support me. I consider myself extremely fortunate to have met all of you. At the same time, I would like to thank the OC Lab members, who always assisted and supported me.

Lastly, I have to present my deep gratitude to my family for providing me with endless support and constant encouragement during my academic career.

This research was supported by Acıbadem Mehmet Ali Aydınlar University Scientific Research Projects Commission (ABAPKO, project no. 2019/04-08) and Scientific and Technological Research Council of Turkiye (TUBITAK, project no. 216S060).

TABLE OF CONTENTS

LIST OF ABBREVIATIONS AND SYMBOLS

ACN	Acetonitrile
ACS	American Chemical Society
Ais	Autoinducers
AMP	Antimicrobial peptide
AMR	Antimicrobial resistance
ANOVA	Analysis of Variance
APNTP	Atmospheric pressure non-thermal plasma
Arg, R	Arginine
ATR/FT-IR	Attenuated total reflection Fourier transform infrared
Boc	*tert*-butoxycarbonyl
ChE	Cholinesterase
Cys, C	Cysteine
DCC	N,N′-dicyclohexylcarbodiimide
DCM	Dichloromethane
DCU	1,3-Dicyclohexyl urea
ddH$_2$O	Double distilled water
DIC	N,N’-Diisopropylcarbodiimide
DMAP	4(dimethylamino)pyridine
DMEM	Dulbecco's modified eagle medium
DMF	Dimethylformamide
DMSO	Dimethyl sulfoxide
EDC	1-[3-(dimethylamino)propyl]-3-ethylcarbodiimide methiodide

EDTA	Ethylenediaminetetraacetic acid
EOs	Essential oils
Et_3N	Triethylamine
FA	Formic acid
FBS	Fetal bovine serum
FDA	Food and Drug Administration
Fmoc	Fluoren-9-ylmethyloxycarbonyl
HPLC	High-performance liquid chromatography
HPMA	2-Hydroxypropyl methacrylamide
LC/MSMS	Liquid chromatography mass spectrometry
Leu, L	Leucine
Mag2	Magainin-2
MAO	Monoamine oxidase
MDR	Multi-drug resistant
MHA	Mueller hinton agar
MHB	Mueller hinton broth
MIC	Minimal inhibition concentration
MRSA	Methilicin-Resistant Staphylococcus
NHS	N-Hydroxysuccinimide
NMR	Nuclear magnetic resonance
PEG	Polyethylene glycol
PEGdiMal	Polyethylene glycol dimaleimide
QS	Quorum sensing

Rbf	Round bottom flask
RNS	Reactive nitrogen species
ROS	Reactive oxygen species
RP-HPLC	Reverse phase high pressure liquid chromatography
SEM	Scanning electron microscopy
SPPS	Solid-phase peptide synthesis
TFA	Trifluoroacetic acid
TIS	Triisopropylsilane
VRE	Vancomycin-resistant Enterococci
WHO	World Health Organization
α	Alpha
β	Beta

LIST OF FIGURES

LIST OF TABLES

ÖZET

İlaç Taşıyıcı Sistemlerin Kombinasyonu ile Yenilikçi Bir Antimikrobiyal Peptitin Kararlılığının Artırılması

Antimikrobiyal direnç (AMR) ile bağlantılı son makalelere göre, AMR kontrol altına alınması gereken küresel çapta bir sağlık problemidir ve bu tehtitin etkisini azaltmak için çeşitli çalışmalar yapılmaktadır. Bu çalışmaların temeli, AMR'yi indüklemeyen ya da etkisiz hale getiren ilaç moleküllerini keşfetmektir. Özellikle antimikrobiyal peptidler (AMP'ler), bu direnç krizine çözüm olarak sunulan en etkili geniş spektrumlu yeni nesil antibiyotikler olarak anılmaktadır. AMP'lerin yüksek antimikrobiyal etkisi, AMR'yi indüklememesi ve doğada da bulunabilirliğinin yanı sıra bazı yan etkilere de sahiptir. Bu yan etkiler düşük ilaç stabilitesi, yüksek toksisite ve hemolitik aktivite, proteolitik degredasyon ve vücutta düşük çevrim süresi gibi etkilerdir. AMP'lerin bu yan etkilerini azaltmak için yeni nesil geniş spektrumlu PEG-AMP konjugatları geliştirdik. Bu nanoyapıların, kimyasal olarak nasıl geliştirildiğini ve *in vitro* deneylerdeki etkinliğini tartışmaktayız. Elde edilen sonuçlara göre geliştirilen altı farklı konjugatın da patojenik veya AMR'ye sahip çeşitli bakteri ve mantarlar üzerinde etkin olduğu kanıtlanmıştır. Ayrıca bu nanoyapılar yüksek stabilite, artmış çözünürlük ve memeli hücrelerine karşı düşük toksiksisite göstermesi gibi özellikleriyle geleceğin umut vadeden yeni nesil geniş spektrumlu peptit antibiyotikleri arasında yer alması olasıdır.

Anahtar Sözcükler: Antimikrobiyal peptit (AMP), Polimer-peptit konjugatı, PEG Polimer, Geniş-Spektrumlu Antibiyotikler, Nanoyapılar

ABSTRACT

Stability Enhancement of a Novel Antimicrobial Peptide with The Combination of Drug Delivery Systems

According to the latest published studies, AMR is a global health problem that needs to be controlled, and various studies are being carried out to reduce the effect of this threat. The basis of these studies is to discover drug molecules that inactivate or non-induce AMR. In particular, antimicrobial peptides (AMPs) are referred to as the most effective antibiotic candidates offered as a solution to this resistance crisis. Besides the high antimicrobial effect, non-induced AMR, and bioavailable nature of AMPs, they also have some adverse effects. These adverse effects are low drug stability, high toxicity and hemolytic activity, proteolytic degradation, and low circulation time in the human body. To reduce these effects of AMPs, we developed a new generation of broad-spectrum PEG-AMP conjugates. We discuss how these nanostructures are chemically developed and their effectiveness in *in vitro* experiments. Six different conjugates developed according to the results obtained have been proven to be effective on various bacteria and fungi that are pathogenic or have AMR. In addition, it is possible that these nanostructures will be among the promising next-generation broad-spectrum peptide antibiotic candidates with their properties such as high stability, increased solubility, and low toxicity to mammalian cells.

Keywords: Antimicrobial peptide (AMP), Polymer-peptide conjugate, PEG Polymer, Broad-Spectrum Antibiotics, Nanostructures

1. BACKGROUND

Conjugation of peptides/proteins having therapeutic properties to polymers to boost their stability and effectiveness as a therapy has been a hot topic in recent years. The solubility, half-life in serum, stability and pharmacodynamic activity of the attached active molecules can be altered based on the chemical structure of the polymer to be utilized. Accordingly, the conjugation of AMPs to long polymer chains has been considered to increase their bioavailability.

In these studies, the usage of the PEG molecule as a polymer with its hydrophilic structure and high stability is quite common. It has also been proven that since it eliminates non-specific protein binding of the side branches of the PEG polymer, it can also inhibit or reduce the attacks of immune system molecules against the therapeutic drug carried by the polymer. Considering all these features, it was decided that the PEG polymer is one of the best biomaterials to reduce the side effects of the AMPs we use. Therefore, three main designs were planned, in which PEG and AMPs were bound in different numbers and structures. Each of these three main designs includes two sub-designs. For this, the peptide sequence was modified with cystine amino acid from the N- or C-terminus and bound to the polymeric structure.

In vitro experiments were performed to understand the changes in toxicity, hemolytic activity, stability, and solubility related with PEG-AMP nanostructures. Thus, it will be possible to determine the effect of its conjugation and to understand from which terminus AMPs are effective and interact.

2. INTRODUCTION AND AIM

This thesis aims to conjugate cathelicidin-like synthetic peptides, whose antimicrobial activity has been proven before, with polymer-based biomaterials to increase their stability and reduce their side effects in a physiological environment.

2.1 Antimicrobial Resistance (AMR)

Antimicrobials such as antifungals, antibiotics, antiparasitics and antivirals are drug molecules used to treat infections in advanced living organisms. Antimicrobial Resistance (AMR) develops when fungi, bacteria, viruses, and parasites evolve over time and no longer react to antimicrobial medications, making infections difficult to treat. This may increase the spread of infection as well as increase the risk of death. Antimicrobial medications lose their effectiveness as a result of antibiotic resistance, making treatment more challenging. AMR is a global health issue, according to the World Health Organization (WHO) (1,2). With the emergence of pathogenic microorganisms that cause AMR and are resistant to antimicrobials by constantly developing novel resistance mechanisms, our ability to treat common infections is declining. Therefore, the rapid spread of superbugs (multi-resistant microbial) that no longer respond to treatment with antibiotics is a global concern. Overuse or misuse of antimicrobial drugs is one of the primary causes of AMR and its fast spread. Following these factors, lack of sanitation and hygiene and unnecessary use of antibiotics in animal husbandry also cause the spread of AMR (1,3,4). What makes the situation worse is that some antibiotics used on livestock are also reserved for the human usage to treat infections caused by end-stage disease or multi-drug-resistant (MDR) pathogens (5). In the coming years, it is estimated that antimicrobial resistance will have a great burden on countries in the fields of economy and health (2). According to the research based on the data collected so far, it is estimated that the death toll from AMR will reach 10 million by 2050 (6), while AMR will cost the global market $100 trillion (7). For all these reasons, there is an urgent need for new antimicrobial drugs. In addition, if individuals do not modify the usage of antibiotics, the fate of the new antimicrobials will be the same as existing antibiotics and become useless.

2.1.1 Classical antibiotics

Antibiotics are antimicrobial agents that are active against microorganisms. Antibiotics are widely utilized in the treatment and prevention of bacterial infections. Antibiotics are classed as "narrow-spectrum" or "broad-spectrum" based on the spectrum of bacteria types they impact. Broad-spectrum antibiotics are effective against a wide range of bacterial types, whereas Narrow-spectrum antibiotics are only effective against some bacteria type (8).

Bacteria can develop antimicrobial resistance against conventional antibiotics by various mechanisms. The resistance can be intrinsic or acquired. Just as there are "intrinsic" mechanisms by which the bacteria can use its genes to survive when exposed to antibiotics, novel mechanisms can also be developed to aid survival using the "acquired" genetic material. The working principle of antibiotics and the main mechanisms developed by bacteria to resist the inhibitory/lethal effects of antibiotics have been revealed (Figure 2.1). Antibiotics are inactivated by enzymes that either degrade or alter the antibiotic molecule. Enzymatic degradation includes the hydrolysis of the antibiotic's functional group (9). Antibiotic-modifying enzymes add different chemical groups to the antibiotic, preventing it from attaching to its target (10,11). Target site modification/mutation can change the antibiotic target to minimize antibiotic binding (12). In target bypass, the function of the antibiotic target is performed by a novel protein that is not inhibited by the antibiotic molecule, rendering the original target insignificant and the antibiotic useless (13). Reduced influx is caused by changes in membrane structure, for instance, the downregulation of porins that allow the passive transport of different compounds, like antibiotic molecules, into the bacteria (14). Transmembrane efflux pumps allow active efflux by exporting antibiotics out of bacteria to lower intracellular concentration (15). Target protection is the physical interaction of a target protection protein with an antibiotic target, relieving it of antibiotic-associated inhibition (16,17).

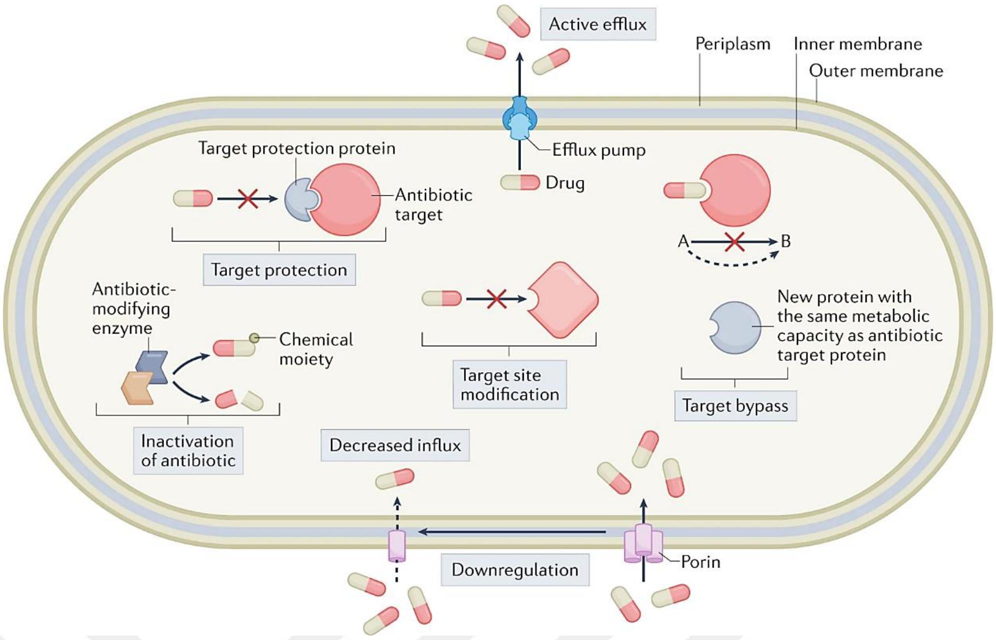

Figure 2.1 A summary of the molecular pathways underlying antibiotic resistance (17).

There have been numerous examples of successful acquisition of these specific resistance genes/mechanisms by worldwide dominant clones of a bacteria species (18,19). Therefore, identifying the resistance genes and developing next-generation approaches against them may be ammunition in our future battle against bacteria.

2.2 Novel Strategies Against AMR

2.2.1 Targeting antimicrobial resistance molecules

2.2.1.1 Enzyme inhibitors

Enzyme inhibitors are synthetic molecules that can either permanently or reversibly reduce or totally suppress enzyme catalytic activity. Examples of inhibitors are monoamine oxidases (MAO) and cholinesterases (ChE) inhibitors applied for a variety of pharmacological applications. Enzymes continue to be ideal targets for drugs because altering an enzyme's chemical function has been demonstrated to improve disease progression. Overall, 47% of all available drugs block enzyme targets (20).

2.2.1.2 Phytochemicals and medicinal plants

Plants synthesize a wide variety of chemicals with a special role to react microbial attack (21). Accordingly, using the antimicrobial and resistance-modifying properties of many different plant extracts and oils, the potential of synthesizing new plant-derived compounds and their use as drug candidates is being evaluated (22).

2.2.1.3 Small molecules

Recent direct-acting small compounds may be developed as improved derivatives of conventional antibiotics or novel chemicals with targeting agent (23). The small compounds can separate three categories: natural compounds, antimicrobial peptides (AMPs), natural chemicals, and inhibitors, like LpxC and LpxA (24).

Antimicrobial peptides (AMPs) are found in nature and have a variety of classes. These small compounds with direct action exhibit broad-spectrum activity, quick and prolonged bactericidal impact, and are highly selective (25). AMPs are often found in the innate immune systems of numerous terrestrial and aquatic species. Thanks to the common acting mechanisms of classical antibiotics, AMPs can target a wide range of bacteria, including Gram-positive and Gram-negative (26,27). Once within the bacterial cell wall, AMPs exhibit further antimicrobial effects by inhibiting protein biosynthesis and nucleic acid synthesis and affecting the cell wall and membrane (28). The inhibitors targeting essential enzymes can be used as a new approach; for instance, LpxC is an enzyme of lipid A production in Gram-negative bacteria strains and a prospective target for novel antibiotics that specifically target Gram-negative infections (29).

2.2.1.4 RNA silencing and gene-editing tools

RNA silencing and gene-editing tools such as crispr-cas system are strategies that potentially enable the production of new antimicrobials. RNA silencing occurs naturally in bacteria and is known to be associated with the regulation of numerous genes. According to the RNA silencing mechanism, the cis and trans sequences in a single mRNA molecule (antisense sequence) fit onto the regulatory regions and thus prevent translation for a while. These antisense sequences can be synthesized synthetically to suppress the translation of bacterial resistance enzymes (30). On the other hand, gene-editing technologies can selectively target bacterial genomes to diminish or eradicate antibiotic resistance and provide new options to treat MDR infections (31,32).

2.2.1.5 Essential oils

Essential oils (EOs) such as terpenes, terpenoids, phenolics, and aldehydes have been found to have antimicrobial properties (33). EOs primarily contribute to bacterial cell membrane rupture and suppression of the efflux pump responsible for some AMR in Gram-negative bacteria (34,35). Recent research has shown that EOs can suppress biofilm formation and quorum sensing (QS) generation while increasing the expression of oxidative stress proteins (36).

2.2.2 Targeting antimicrobial resistant bacteria

2.2.2.1 Bacteriocins and lantibiotics

Lantibiotics are classified as type A and type B peptides. Type-A lantibiotics are cationic peptides with up to 34 residues that are homologous in the organization of their Lan bridges. These peptides, which include nisin, epidermin, and subtilin, typically damaging the bacterial membrane integrity. Type-B peptides are globular, with up to 19 residues, and the peptides act thanks to inhibition enzyme activity, for instance, by inhibiting cell wall synthesis (37).

Bacteriocins are peptidic toxins or proteinaceous generated by bacteria and are type-A lantibiotics. These chemicals can inhibit or kill closely associated or irrelevant bacterial strains while not harming the original bacteria due to particular immune proteins. In addition, bacteriocins have a wide range of structures and activity, and are extremely heat stable (38).

2.2.2.2 Insect derived enzymes and AMPs

Insect-produced AMPs are smaller in size and include cationic-charged amino acids. Based on their amino acid sequence and structure, insects' AMPs divide into four types of AMPs; Proline-rich peptides, alpha-helical peptides, cysteine-rich peptides, and glycine-rich proteins (39). Insect innate immunity consists of cysteine-rich peptides, which are renowned for their potential to suppress biofilm development (40). Peptide-membrane contact directly increases antibacterial and antibiofilm activity.

2.2.2.3 Probiotic bacteria and coinfection strategy

The administration of microbes and the acceptance of coinfection techniques with probiotic benefits is gaining appeal as a complementary strategy to prevent the spread of AMR infections in medicine (41). Probiotics are living bacteria that can provide health benefits when consumed. Probiotics' effectiveness in combating AMR is based on their ability to avoid the direct selection pressure put by antibiotics on pathogenic microbes. Probiotics inhibit infection through a range of ecological processes, including competition for the ecologic gap, colonization resistance as the synthesis of AMPs with bactericidal action (42). Furthermore, probiotic treatment has been connected to a considerable decrease in antibiotic usage as a decrease in the selective pressure related to traditional therapeutic approaches (43).

2.2.2.4 Using of monoclonal antibodies

Monoclonal antibodies are pharmacological compounds with a high level of specificity. Monoclonal antibodies produced for bacterial infections generally target surface-exposed antigens and toxins that are untargeted by antimicrobials and are improbable to be influenced by available resistance mechanisms. In the battle to confront the worldwide challenge of antibiotic resistance, therapeutic antibodies are being developed as an alternative method since they have potential benefits over broad-spectrum antibiotics (44,45).

2.2.2.5 Bacteriophage therapy

Bacteriophages are viruses that infect archaea/bacteria. The two species have a parasitic relationship in which the bacteriophages employ the host's biosynthetic machinery to produce key components like lipids and proteins required for phage capsid development and replication stage (46). These organisms, despite their appearance, are not dangerous to people/animals and can be employed to cure bacterial infections.

2.2.2.6 Biofilm dispersion

Biofilm is a survival strategy and adaptability. Typically, biofilm formation is the underlying cause of antibiotic administration failure, accounting for 65%-80% of all infections. There are two types of biofilm dispersion mechanisms: active and passive dispersion. The generation of enzymes that break down the biofilm matrix and assist dispersion is reliant on a decrease in intracellular c-di-GMP levels, which results in active dispersion. Passive dispersion is based on initiates that directly leave cells from the biofilm (47,48). Both intracellular c-di-GMP signaling, and intercellular QS signals are crucial in biofilm formation in this regard. The interaction of these signaling pathways is being studied to find new ways that inhibit or reduce biofilm formation.

2.2.2.7 Anti-persister antimicrobials

Bacterial cells that, after exposure to antibiotics, cause the formation of treatment-resistant bacterial subpopulations only through adaptation, without generating antibiotic-resistant mutations, are called persister cells. Bacterial persistence is related to an increased risk of AMR during therapy because persister cells, which can induce recolonization and relapse following antibiotic usage, eventually contribute to repeated resistant infections. One strategy for combating AMR might be the discovery of new compounds having anti-persister activity (49,50).

2.2.2.8 Disruption of QS

Biofilm production and QS are closely related activities. QS is a cell-to-cell communication pathway that controls and harmonizes gene expression (51). Autoinducers (Ais) are signaling molecules that bacteria employ to coordinate gene expression, pathogenicity, and biofilm formation. Bacteria employ QS inhibitors and quorum quenching enzymes to regulate Ais and destroy signaling molecules. The application of quorum-quenching compounds can regulate microbial quorum induction, resulting in a decrease in pathogenicity, biofilm development, and microbial infections (52,53).

2.2.3 Drug delivery systems (DDS)

It is known that drug delivery systems improve the treatment process from many aspects as increasing targeting properties and therapeutic efficacy, reducing toxicity, and increasing biocompatibility. As the therapeutic environment shifted from small-molecule pharmaceuticals to a next generation of treatments such as monoclonal antibodies, proteins, nucleic acids, peptides, and even living cells, drug delivery methods adapted to match their specific delivery requirements (54). Especially recently, combinations of drug delivery systems with antimicrobial agents have been studied. The progress of antimicrobial delivery systems is promising news for increasing antibiotic cell permeability, which is one of the hurdles in antibiotic research (55). Using bacterial iron transport mechanisms is a significant strategy to increase antimicrobial activity. When combined with antibiotics, synthetic siderophores analogs can operate as a delivery vehicle, promoting antibiotic entry into bacteria. The combination of siderophore with ampicillin was found to boost action against *Pseudomonas aeruginosa (P. aeruginosa)* 1000-fold and gram-negative enterobacteria 100-fold. Scientists also proved that the combination of siderophore and ampicillin was not a substance for *P. aeruginosa's* efflux pumps, allowing them to avoid one of the essential AMR mechanisms in these bacteria (56).

Another approach, polymeric nanoparticles are developing as a technique for improving bioavailability, drug solubility circulation time, and stability while at the same time decreasing microbiota exposure to non-lethal concentrations that can contribute to AMR development. Most Polymeric nanoparticles allow for sensitive drug release via various methods, such as elution, diffusion, chemically or stimuli-controlled, and these nanoparticles are made from natural products like collagen, chitosan, or gelatine, making them less toxic and biocompatible biomaterial. Also, synthetic materials like polyethylene glycol (PEG) and polylactic acid can be used for nanoparticles. The ability of improved phosphatidylcholine-chitosan combines nanoparticles coated with gentamycin to prevent biofilm and bacterial growth in Gram-positive and Gram-negative bacteria was demonstrated (57,58).

Nanovesicles, such as polymeric nanoparticles, metallic nanoparticles, carbon nanotubes, dendrimers, and liposomes are commonly used to create nanocarriers. Liposomes, which are lipid-nano particles constituted of a concentric phospholipid bilayer and a biodegradable nanostructure, can deliver both hydrophobic and hydrophilic medications because of their exterior liposomal bilayer and posterior interior aqueous part (59,60). Some liposomes, like polyvinyl-pyrrolidone-iodine hydrogel, are now available on the world market as topical medication with action against a broad-spectrum of bacterial strains for usage on exterior wounds (61). This approach allows dosage regulation at concentrations higher than the MIC values while decreasing dose-dependent toxicity (60,61). Liposomes were also shown to boost antibacterial activity against *Acinetobacter baumannii* (*A. baumannii*), *Escherichia coli* (*E. coli*), *P. aeruginosa*, and *Klebsiella pneumoniae* (*K. pneumoniae*) by entrapping polymyxin B in 1,2-dipalmitoyl-sn-glycero-3-phosphocholine and cholesterol (DPPC/Chol) liposomes (62).

In the same concept, peptides, proteins, or monoclonal antibodies can conjugate and convert into antimicrobial nanostructures. Although antibody-drug conjugates are mostly used for cancer studies, antimicrobial antibody-drug conjugates have been started to be studied recently. These conjugates include an antibiotic molecule/antimicrobial agent covalently bound with a monoclonal antibody. The antibody-drug conjugate DSTA4637S, a novel THIOMABTM IgG antibody bound with rifamycin class antibiotic by a protease cleavable linker, is currently being studied in preclinic as a potential treatment for complex S. aureus infection causing bacteriemia (63).

2.2.4 Physicochemical methods

2.2.4.1 Atmospheric pressure non-thermal plasma (APNTP)

Non-thermal (or cold) plasma at atmospheric pressure is a novel technology that is being studied for its antimicrobial capabilities. *In vitro* testing of APNTP for various microorganisms revealed that it is efficient in the inactivation of fungi, bacteria, parasites, and viruses. The precise mechanisms of APNTP-based bacterial inactivation are unknown. However, it appears to be effective via produced products like reactive oxygen species (ROS), UV light, reactive nitrogen species (RNS), and charged particles inside a plasma gas phase (64,65). Importantly, Gram-negative bacteria were shown to be more susceptible to APNTP than Gram-positives, indicating that APNTP-promoted cell wall and membrane destruction is a crucial element (66). APNTP may provide the benefit of inactivating bacteria without harming mammalian cells (67,68).

2.2.4.2 Photoinactivation

Photoinactivation is a promising technique for eradicating pathogenic bacteria that uses a photosensitizer-chromophore, visible light, and molecular oxygen to generate ROS, which causes bacterial death. Photoinactivation has been shown to function on a diverse variety of bacteria, including susceptible and antibiotic-resistant strains, and with these features, photoinactivation can be an alternative therapy against AMR (69,70).

2.2.4.3 Sonodynamic Therapy

Sonodynamic therapy is related to the synergistic impact of ultrasound and a chemical molecule known as a sonosensitizer, in which an inaudible sound with a frequency less than 20 kHz can kill bacteria (71,72). Sonodynamic therapy employs a non-toxic sonosensitizer, molecular oxygen, and relatively low-intensity ultrasound to sensitize the target location, which may cause micro-bubbles via acoustic cavitation during contact between the target cells and ultrasonic waves. The potential of ultrasound to increase bacterial absorption of antibiotics without radiation is well known (73). As a result, the Sonodynamic therapy-Classical antibiotic combination can be a solution for some AMR issues (74).

2.3 Antimicrobial Peptide (AMP)

Antimicrobial peptides (AMPs) are helping molecules in nature. They are produced by microorganisms to defend themselves against competitors or hosts. AMPs generally consist of 10–50 amino acids. Natural AMPs have unique properties such as water soluble, positively charged, and amphiphilic sequence (75). Basically, AMPs can be categorized into three groups depending on their secondary structure: α-helical; β-sheet; and extended AMPs (76).

AMPs are potential future antibiotics because of their multifunctional and broad-spectrum activities. This spectrum includes fungi, parasites, encapsulated viruses, Gram-positive and Gram-negative bacteria, and even multi-drug resistant bacteria (77). In addition, the possibility of AMPs developing resistance against microorganisms is very low compared to conventional antibiotics (78). All these benefits make AMPs ideal candidates for pharmacological medications.

2.3.1 Mechanism of AMP

Properties of AMPs, such as hydrophobicity, charge, size, secondary structure, and amphiphilic characteristic can affect specificity and antimicrobial activity. AMPs can permeabilization of membranes and/or influence intracellular function (79).

Disruption of bacterial membrane integrity is the main target of AMPs. Many different models have been described that disrupt the integrity of the membrane by causing osmotic lysis (80,81). According to the "barrel-stave" model, peptides penetrate the membrane and drive their hydrophobic portions toward the bilayer's lipid core, generating a transmembrane pore. The "toroidal pore" concept proposes that AMPs enter perpendicularly into the bacterial membrane via interactions between the hydrophilic portion of the AMPs and the lipid bilayer of the membrane. As a result, the membrane bends and generates a "toroidal pore" (82). The "carpet model" is a non-pore-producing AMP mechanism. Instead, attach to the hydrophobic core of the bacterial membrane, the peptide positions itself parallel to the bacterial membrane and coats it as a carpet. The shape and fluidity of the membrane are distorted by a strong electrostatic interaction between the cationic peptide and negatively charged phospholipid groups of the membrane. When the peptide reaches its limit, membrane disruption or cell lysis is initiated (83,84). The “aggregate or detergent” model suggests the generation of aggregates of lipids and AMPs, allowing the translocation of the peptides across bacterial membranes. The peptides form micelles with a fragmented membrane like a detergent.

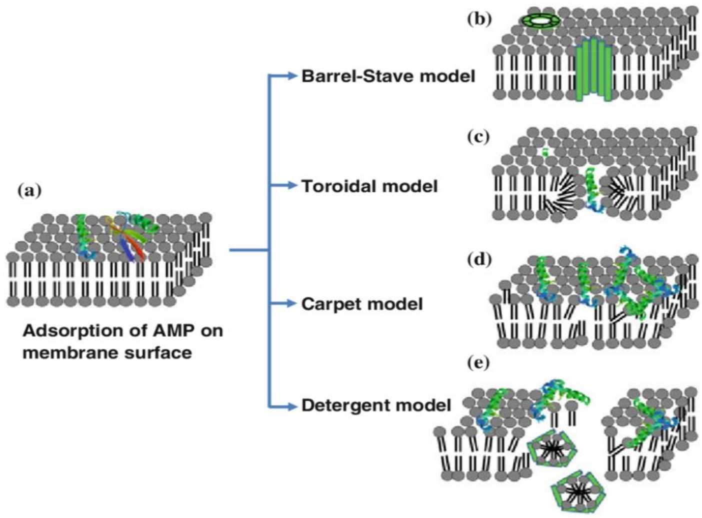

Figure 2.2 Different models of membrane permeabilization by AMPs (83). (a) Inserting of AMPs on the bacterial membrane, (b) Barrel-Stave model, (c) Toroidal model, (d) Carpet model, (e) Detergent model. The green-blue colors represent the AMPs, while the grey color shows the bacterial membrane.

A few peptides pass the cytoplasmic membrane and target pathogen-essential cellular functions, including nucleic acid biosynthesis, DNA replication, LPS binding proteins, cell division, protein synthesis, and metabolism (85). Because of their affinity for negatively charged phosphodiester linkages, several cationic AMPs have been demonstrated to bind and flocculate nucleic acids or related anionic molecules (86,87). AMPs are well known for their antibacterial actions, but they also have immunoregulatory roles. As a result, they can help to attract and activate immune cells. Cathelicidin BF, for instance, has been demonstrated to have an immunomodulatory activity that can alleviate *P. aeruginosa* pneumonia in mice (88).

AMPs can inhibit several phases of biofilm development. Some AMPs have been shown to hinder bacterial adherence to surfaces by lowering specific forms of swimming/swarming motility. They can also induce twitching known as a motility to enhance biofilm breakdown. AMPs can also suppress the expression of specific genes involved in QS (89). For example, LL-37 cathelicidin has been shown to target QS pathways that govern *P. aeruginosa* biofilm development (26,90).

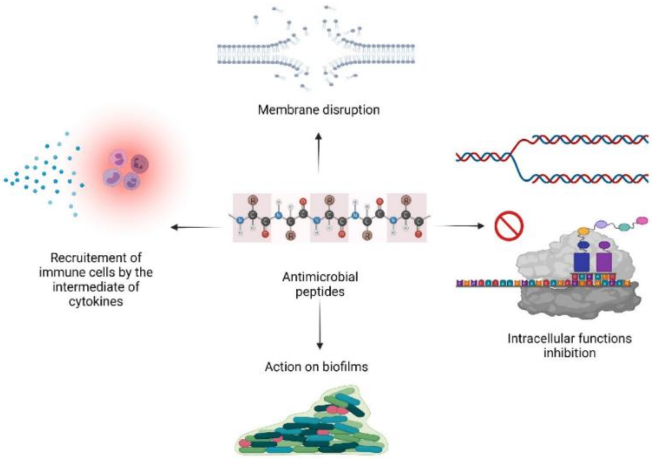

Figure 2.3 AMPs’ mechanisms of action (26).

2.3.2 Production of AMP

Three strategies generally use for AMPs production: recombinant expression, cell-free protein synthesis, and chemical synthesis (91,92).

Recombinant expression enables the production of peptides/proteins in living organisms such as bacteria, yeast, and mammalian cells. Peptide production in different organisms primarily depends on the properties and structure of the peptide. For instance, several peptides may be better produced in bacteria, while others may be more suited for production in mammalian cells. Bacteria are one of the most used microorganisms in the recombinant production of peptides. Bacterial cells are used due to their cheap, fast, and simple production process. *E. coli*, which is one of the microorganisms with the most recombinant expression studies, is a bacterium that is frequently used in the production of peptides (93). Plasmids containing peptide genes are used for production in bacterial cells. However, during this production, the toxic effect of AMPs on the host and the sensitivity of bacteria to protease enzymes are the biggest problems in recombinant production (94). In addition, compelling purification processes can reduce the efficiency of production. In yeasts, *Saccharomyces cerevisiae* (*S. cerevisiae*) and *Pichia pastoris* are the most used yeast species for peptide production. Yeasts can perform some post-translational modifications and provide high-efficiency peptide production (95,96). However, yeasts have a more expensive production process than bacteria. Mammalian cells are another option for the recombinant production of AMPs. In fact, mammalian cells are cells that naturally produce AMPs. Therefore, the production of AMPs in this process is closer to natural production methods (97). However, production of AMPs in mammalian cells can be more time-consuming and expensive than in other organisms due to their growth conditions.

Peptides can be produced by cell-free protein production method without using living cells. In this method, peptide/protein production is performed by isolating the components of cell mechanisms (ribosomes, tRNAs, amino acids, etc.) responsible for protein synthesis (98). This method has many advantages for AMPs. First, this method makes complex processes such as cell culture and gene transfer unnecessary for AMP production. Second, it provides high efficiency for production with no additional host proteins. Third, since there are no purification steps as in recombinant production, it is carried out quickly (99). Cell-free protein production of AMPs can be accomplished using different cell systems. For example, *E. coli*, *S. cerevisiae*, and several types of cell lysates can be used (100). In addition, cell-free production of AMPs can also be produced by commercial kits with an *in vitro* synthesis system (101).

Peptides can be produced using the solid phase peptide synthesis (SPPS) method, which is the most widely used and automated method in chemical synthesis. The SPPS method provides extension by adding amino acid units to the peptide chain, using a starting amino acid attached to a solid support (102). This method enables the production of peptides of high purity and high efficiency.

Fluorene-methyloxymocarbonyl (Fmoc) and *tert*-butoxycarbonyl (Boc) methods are protective groups commonly used in the synthetic production of peptides. In the Boc method, free amine groups of amino acids are protected by Boc groups. The peptide chain is formed and last all Boc groups are removed. In the Fmoc method, the peptide chain is first combined with the free amine group on the solid support to which it is attached. The peptide chain is then formed by adding amino acids in ascending order. Before each added amino acid, the N-terminal Fmoc group is used to protect the amine group. Next, the Fmoc group is removed, and the amine group is reacted with the next amino acid to obtain the desired peptide sequence (103). The Fmoc method is more widely used than the Boc method because the Fmoc groups can be removed more easily and faster than Boc groups, and it is less toxic (104). In addition, the purity of the peptides produced by the Fmoc method is generally higher. In addition, the Fmoc protective group is optimized to suit the high-speed manufacturing processes used in SPPS devices.

2.3.3 Limitations of AMP

An incoherence was seen between the synthesized AMPs and the results in clinical trial findings, although AMPs are known as promising compounds against AMR. Enzymatic cleavage, instability, short circulation time, immunogenicity, and toxicity to healthy human cells are among the limits of AMPs. These variables reduce the bioavailability of AMPs, causing reduced therapeutic potential. Peptidomimetic methods such as glycosylation, lipidation, grafting, cyclization, PEGylation, D-amino acid insertion, dendrimers, and stapling are potential strategies for next-generation AMPs (105).

2.4 Conjugation Strategies

Bioconjugation strategies have been developed to create an efficient drug delivery system by covalently linking two molecules to form a wide range of hybrid nanostructures (106). A biomolecule or a biomolecule recognition element can be present in at least one molecule. The function of the other molecule according to the goal of bioconjugation. Further, the second molecule may be a drug or polymer with the ultimate aim is targeting and/or dynamic or pharmacokinetic regulation (107). At the same time, bioconjugation is a type of functionalization that tries to boost stability, reduce toxicity, preserve the drug from protease activity and promote the delivery system's targeting capabilities (108,109).

The correct linker can provide the bioconjugate system with new functionalities and smart properties. Bioconjugation reactions are grouped by the reactivity or functional group present in the related conjugation strategy, such as thiol reactions, hydroxyl reactions, amine reactions, active hydrogen reactions, aldehyde and ketone reactions, carboxylate reactions, cycloaddition reactions, or photochemical reactions (109).

There are three main application areas in synthetic bioconjugation techniques: nanoparticles-based conjugates, antibody-radionuclide conjugates, and antibody–drug conjugates like polymeric, peptide-based, and peptidomimetic. Bioconjugates have been proposed for a broad spectrum of biological applications, involving biological tests, medication and gene delivery, imaging, and biosensing (110). The development of monoclonal antibodies and recombinant DNA technologies has resulted in a biotechnological evolution that has resulted in an increasing number of antibody-based drugs, peptides, and proteins. However, most of peptide/protein-based technologies have limitations in clinic due to their unforeseeable low therapeutic activity. So, sometimes regular administration at an exorbitantly high dose is necessary to demonstrate their therapeutic activity in vivo. Therefore, homeostasis is disrupted, and unexpected adverse effects occur. The bioconjugation strategy with water-soluble polymers promotes the body distribution and plasma clearance, causing increased therapeutic activity and reduced adverse effects (111).

2.4.1 PEGylation strategy

Polymers used in drug conjugations are extremely versatile due to their chemistry and structure. Among the most extensively used biocompatible linear polymers are N-(2-Hydroxypropyl) methacrylamide (HPMA) and poly (ethylene) glycol (PEG). PEGylation is the covalent conjugation of biological molecules with PEG polymer, a non-immunogenic, non-toxic, and is utilized as a technique to alleviate problems related to various biopharmaceuticals. PEGylation strategy alters the biological molecule's physical and chemical characteristics, such as electrostatic binding, conformation, and hydrophobicity, causing an enhancement in the drug's pharmacokinetic behavior (112). PEGylation enhances drug solubility, increases drug stability and circulation time in blood, and decreases immunogenicity, protease activity, and renal excretion, allowing for lower dose frequency (113,114). A range of therapeutic peptides, proteins, and antibodies, as well as small molecules, have been PEGylated to benefit from these positive pharmacokinetic effects. The FDA has authorized many PEGylated proteins for clinical use, including PEG-granulocyte colony-stimulating factor (Neulasta) (115), PEG-interferon-2a (Pegasys) (116), PEG-growth hormone receptor antagonist (Somavert) (117), and PEG-interferon-2b (PEG-Intron) (118). Many more PEGylated peptide/protein conjugates are predicted to be developed and marketed worldwide in the future.

3. MATERIALS AND METHODS

3.1 Materials

Chemical synthesis and purification/analysis: 1-[3-(dimethylamino)propyl]-3-ethylcarbodiimide methiodide (EDC), N,N′-dicyclohexylcarbodiimide (DCC), 4(dimethylamino)pyridine (DMAP), triethylamine (Et_3N), anhydrous dimethylformamide (DMF), diisopropylcarbodiimide (DIC), anhydrous N-Hydroxysuccinimide (NHS), trifluoroacetic acid (TFA), Oxyma®, piperidine, dichloromethane (DCM), acetonitrile (ACN), toluene, amyl acetate, ethyl alcohol, propylene and uranyl acetate were purchased as American Chemical Society (ACS) grade from Sigma-Aldrich, USA.

In vitro experiments: Mueller–Hinton agar (MHA, Oxoid), Mueller–Hinton broth (MHB, Oxoid), dimethyl sulfoxide (DMSO, Sigma-Aldrich), Triton X-100 (Sigma Aldrich), fetal bovine serum (FBS, ATCC 30-2020™), penicillin-streptomycin (Pen/Strep, Gibco™), Dulbecco's modified Eagle's medium (DMEM, Gibco™), and protease inhibitor (cOmplete^{TM} Mini Protease Inhibitor Cocktail, Roche) were used.

3.2 Thiolated Peptide Synthesis

To functionalize the peptides, versions of the peptide in which the cysteine is located at the N-Terminal or C-Terminal of the peptide, respectively, were synthesized. Functional thiolated peptides were chemically synthesized using solid phase peptide synthesis (SPPS) device (CEM, Liberty ™ Blue and CEM Discover ™) following standard Fmoc protocol. Rink Amide (0,70 mmol/g loading capacity) resin was used for the synthesis of amide end peptides from C-terminus. The synthesis scale was determined as 0,10 mmol and 0,143 mg Rink amide resin was weighed for this scale. Before synthesis, resin was kept in DMF solvent for 30 min to 1 h to swell. All amino acids were used 0,2 M and L-form conformation. For synthesis, 3,12 gr Arginine (Arg) in 24 mL DMF, 0,36 gr Cysteine (Cys) in 3mL DMF and 1,49 gr Leucine (Leu) in 21 mL DMF were prepared.

In the SPPS, peptides are synthesized to extend from the C-terminal to the N-terminal. Amino acids and resin have protecting groups to prevent undesirable side reactions during synthesis. In the initiative step (resin loading) of the synthesis cycle, first amino acid (in DMF) was anchored to resin from C-terminal after removing the functional deprotection group of the resin. The anchored peptide is extended by repetitive cycles which include deprotection and coupling steps. In the deprotection step, Fmoc protecting group was removed from N-terminal of amino acid with the help of 20% piperidine in 65 mL DMF. In the coupling steps of cycle, it is attached from the C-terminus carboxyl group of the newly added second amino acid to the N-terminal amine group of the previous amino acid, using 1,0 M Oxyma® (in 10 mL DMF) and 0,5 M DIC (in 20 mL DMF) as activator base and activator, respectively.

In the last phase of the synthesis consists of two steps: N-terminal deprotection, cleavage & side-chain deprotection. Firstly, the N-terminal Fmoc protecting group of the amino acid at the end of the peptide sequence was removed. For the second step, the peptide sequence is released from the resin support with using peptide cleavage system (CEM, Razor^{TM}). The final product, which was transferred to the cleavage filter before the cleavage step, was washed three times with DCM and then incubated with cleavage cocktail at 38°C for 35 min. The cleavage cocktail contains 125 µL of double distilled water (ddH_2O), 125 µL of triisopropylsilane (TIS) and 4,75 mL of trifluoroacetic acid (TFA). Also with this cocktail, side-chain deprotection is provided. The cleaved crude peptides were precipitated in cold diethyl ether (−20°C) and centrifuged at 4500 rpm for 3 min. After centrifugation diethyl ether and cleavage cocktail were carefully discarded, and this step was repeated two times more with cold diethyl ether. Peptides were left to dry under vacuum.

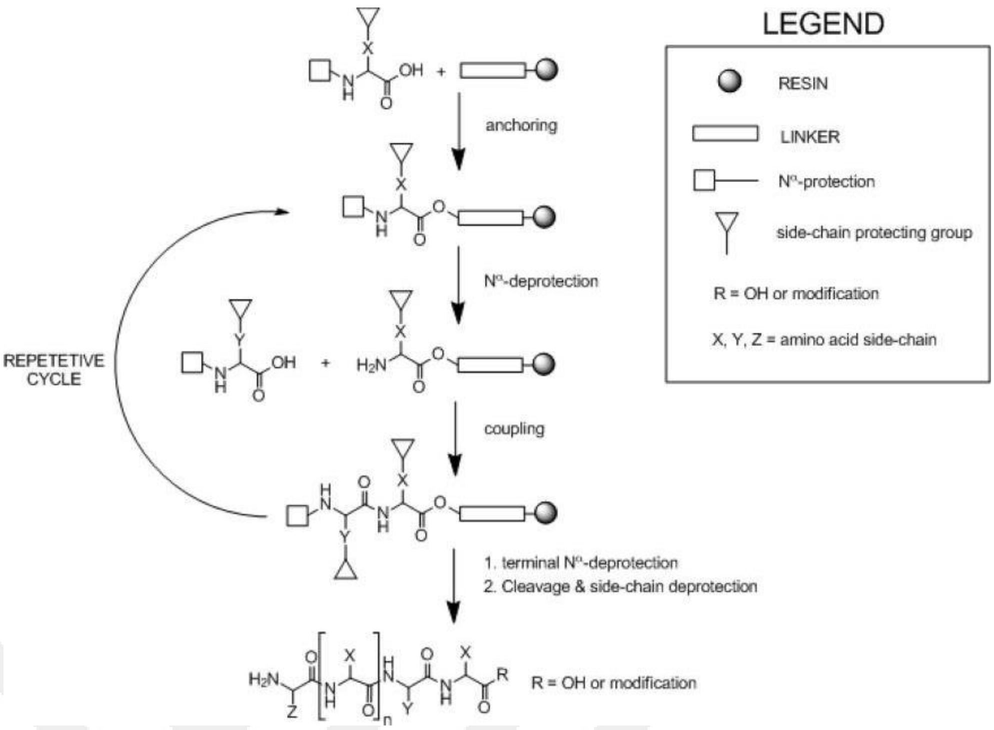

Figure 3.1 SPPS stages (119).

Table 3.1 Sequences of synthesized thiolated peptides.

Modified Peptide	Peptide Sequence	Modified Peptide Sequence	Peptide Model
C-TN6	RLLRLLLRLLR	C-RLLRLLLRLLR	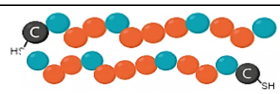
TN6-C	RLLRLLLRLLR	RLLRLLLRLLR-C	

Table 3.2 Physical properties of synthesized thiolated peptides.

Modified Peptide	pI	Net charge at pH 7.0	Molecular Weight (g/mol)	Ratio of Hydrophilic Residues
C-TN6	12,97	4,95	1537,04	33%
TN6-C	12,97	4,95	1537,04	33%

3.3 Purification and Analysis of Thiolated Peptides

3.3.1 HPLC

Synthesized modified peptides (C-TN6 and TN6-C) were dissolved in 50% acetonitrile (ACN) to have a concentration 1,5 mg/mL. By using HPLC (260 Infinity Quaternary Liquid Chromatography systems, Agilent Technologies) with the help of C-18 column (RPC 250 x 10 mm ID hydrophobic 6 µm, Agilent VariTide), the modified peptides were purified and analyzed. UV absorption at 214 nm and 280 nm was used to detect peptide peaks. At 2 mL/min flow rate, ddH_2O (include 0,05% TFA) and acetonitrile (ACN, include 0,025% TFA) were used as mobile phases A and B for the system, respectively.

At first, synthesized thiolated peptides were scanned in a range of 0–100% B solution for 30 min in a linear gradient. Subsequently, a special method was applied for purification according to the position of the peptide peak (retention time in B%) on the chromatogram. For purification, the column was equilibrated by 0% B mobile phase. The same purification methods were used for both TN6-C and C-TN6.

To obtain pure sample, proper peaks were collected from fraction collection after repetitive purification steps. Then, all samples were frozen (–80°C) and lyophilized using Freeze Dryer (Labconco).

To analyze the purity of the collected peaks, approximately 1 mg of dried samples was weighed and dissolved in 1 mL of 50% ACN. The column was equilibrated by 5% B mobile phase for analysis. The same analysis methods were used for both TN6-C and C-TN6 (Table 3.3).

Table 3.3 prep RP-HPLC analysis of thiolated peptides.

Method	
Time (min)	B solution (%)
0–5	5%
5–35	5–80%
35–35.01	80–100%

3.3.2 LC/MSMS

The purified peptides were analyzed by LC/MSMS (6420 Triple Quad LC/MS, Agilent Technologies). While creating the method, MS2scan method was used. Samples were analyzed for 1 min at 135 V between 500–2200 Da.

3.4 Polymer-Peptide Conjugates Synthesis

3.4.1 PEG-pep conjugate synthesis

Table 3.4 Reaction table for PEG-pep**.**

Chemical	**Equivalent**	**Molecular Weight**	**Mol (mmol)**	**Weight (mg)**	**Volume (mL)**	**Density (g/cm^3)**
Linker (Mal-PEG_6-NHS ester)	1	601,60	0,008311	5,00		
PEG (2K)-NH_2	1,15	2000,00	0,009558	19,12		
Thiolated peptide	1,1	1537,03	0,009142	14,05		
Et_3N	2	101,19	0,020778	1,68	0,0023	0,73
DMF-anhydrous					2,00	
Product:		4023,54				

All calculations in the reaction table (table 3.4) are based on the use of 5 mg of the hetero-functional linker molecule (Maleimide-PEG_6-NHS ester, Sigma Aldrich, MW: 601,6 g/mol). This linker has a carboxylic acid group (NHS-activated) at one end and a functional maleimide group at the other side. For the synthesis of PEG-peptide conjugates, C-TN6 and TN6-C (MW: 1537,03 g/mol) peptides were used, respectively.

The reaction was planned in two steps. In the first step, the Thiol group of the peptide was turned into a better nucleophile by leaving its hydrogen in the basified medium with Et_3N (Triethylamine, Sigma-Aldrich, MW: 101,19 g/mol) and reacted (1,4-Michael addition reaction) with the functional maleimide group in the structure of the linker molecule to bind peptide and linker molecule. In the second step, an amide bond was formed because of the attack of the functional amine group from one end of the PEG (Methoxy-PEG amine, Sigma Aldrich, MW: 2000 Da) to the carboxylic acid (activated by NHS).

Linker molecule, peptide, and Et_3N in the calculation indicated in table 3.4 were added to the round bottom flask (rbf), respectively, and mixed using a magnetic stirrer at room temperature for 2 h in anhydrous DMF (Sigma Aldrich) to initiate the "1,4-Michael addition reaction". Afterward, pre-dissolved PEG in anhydrous DMF was added to the reaction mixture and stirred at room temperature overnight. All experimental steps were carried out under nitrogen gas.

3.4.2 PEG-(pep)$_2$ conjugate synthesis

Table 3.5 Reaction table for linker activation.

Chemical	Equivalent	Molecular Weight	Mol (mmol)	Weight (mg)	Volume (mL)
Linker (Bis-Mal-Lysine-PEG$_4$-acid)	1	695,70	0,028748	20,00	
EDC	1,5	191,70	0,043122	8,27	
NHS	1,2	115,09	0,034498	3,97	
DMF-anhydrous					1,00
Product:		792,79			

Table 3.6 Reaction table for PEG-$(pep)_2$.

Chemical	Equivalent	Molecular Weight	Mol (mmol)	Weight (mg)	Volume (mL)	Density (g/cm^3)
Linker-NHS	1	792,79	0,003784	3		
PEG (2K)-NH_2	1,25	2000,00	0,004730	9,46		
Thiolated peptide	2,1	1537,03	0,007947	12,1		
Et_3N	2	101,19	0,007568	0,77	0,001	0,73
DMF-anhydrous					2,00	
Product:		5751,76				

Trifunctional linker molecule (Bis-Mal-Lysine-PEG4-acid, BroadPharm, MW: 695,7 g/mol) (table 3.5) has a carboxylic acid group not activated by NHS at one end and functional maleimide groups at the other two ends on the same side.

For the synthesis of PEG-$(pep)_2$ conjugates, C-TN6 and TN6-C (MW:1537,03 g/mol) peptides were used, respectively. Thiolated peptides were used at approximately 2 times the equivalence of the number of peptides used in the PEG-peptide conjugate (Table 3.6).

The conjugation reaction was planned in three stages. Firstly, NHS (Sigma-Aldrich, MW: 115,09 g/mol) was attached by activating the carboxylic acid end of the trifunctional linker molecule with EDC (Sigma Aldrich, MW: 191,7 g/mol). At the second step, the two ends of the trifunctional linker molecule containing maleimide were bonded by reacting from the thiol end of the peptide molecules with the help of Et_3N. As a last step, the amine group of the PEG polymer was attached to the activated end of the trifunctional linker molecule with Et_3N.

To activate the trifunctional linker molecule by NHS, all the materials in table 3.5 were mixed and reacted on a magnetic stirrer for 1 day. The next day, the NHS-activated trifunctional linker was precipitated and left to dry under high vacuum. Then, except the PEG polymer, all the materials in table 3.6 were added in a new rbf and left on the magnetic stirrer for the 1,4-Michael addition reaction. After 2 h, the PEG polymer was added, and left for 2–3 days. All reactions were carried out at room temperature and in nitrogen gas.

3.4.3 pep-PEG-pep conjugate synthesis

Table 3.7 Reaction table for the PEG-linker synthesis.

Chemical	Equivalent	Molecular Weight	Mol (mmol)	Weight (mg)	Volume (mL)
OH-PEG (2K)-OH	1	2000,00	0,10	200,00	
Linker (6-Maleimidohexanoic acid)	2,4	211,21	0,24	50,70	
DCC	2,64	206,33	0,26	54,50	
DMAP	1,2	122,17	0,12	14,70	
DCM-anhydrous					10,00
Product:		2420.6			

Table 3.8 Reaction table for pep-PEG-pep.

Chemical	Equivalent	Molecular Weight	Mol (mmol)	Weight (mg)	Volume (mL)	Density (g/cm^3)
PEGdiMal	1	2420,60	0,005371	13,00		
Thiolated peptide	2,5	1537,03	0,013426	20,64		
Et_3N	2	101,19	0,010742	1,09	0,0015	0,73
DMF-anhydrous					1,20	
Product:		5495,2				

pep-PEG-pep reaction consists of 2 steps: PEG-linker synthesis (PEGdiMal) and peptide addition. At the first step in the production of PEG-linker, possible water molecules that can be found in the PEG polymer were removed with the help of anhydrous toluene. For this, 200 mg PEG polymer was weighed, and dissolved in 50 mL toluene. Afterwards, the toluene was removed by the evaporator and the remaining solid was left to dry under high vacuum. As a second step, the materials in table 3,7 were added to rbf and kept in the reaction for 2–3 days. All reactions were carried out at room temperature and in nitrogen environment. After the reaction, dichloromethane (DCM) was removed. The remaining solid was dissolved in 20 mL ethyl acetate. DCC (N,N′-Dicyclohexylcarbodiimide, Sigma Aldrich, MW: 206,33 g/mol) which is added during the reaction, turned into DCU by collecting water molecules from PEG (Sigma Aldrich, MW: 2000 Da), DMAP (4-(Dimethylamino)pyridine, Sigma Aldrich, MW: 122,17 g/mol) and 6-Maleimidohexanoic acid (Sigma Aldrich, MW: 211,21 g/mol). To remove DCU, pore size: 4 isocam filter was used. Ethyl acetate from the filtered sample was suspend by evaporator and dissolved in DCM (Sigma Aldrich). Then, by applying the precipitation method, it was kept at –20°C, overnight. The last step of

PEG-linker production, the precipitated solution was filtered, the remaining solids were dissolved in DCM again and filtered. DCM was removed from the obtained solution by evaporator and the remaining solid was left in high vacuum overnight.

For the synthesis of pep-PEG-pep conjugate, C-TN6 and TN6-C (MW:1537,03 g/mol) peptides were used, respectively. Thiolated peptides were used at approximately two times the equivalence of the number of PEGdiMal molecule. Then, except the PEGdiMal molecule, all the materials in Table 3.8 were added in a new rbf and left on the magnetic stirrer for the 1,4-Michael addition reaction. After 20 min, PEGdiMal molecule was added, and the reaction left for 2–3 days. All reactions were carried out at room temperature and in nitrogen gas.

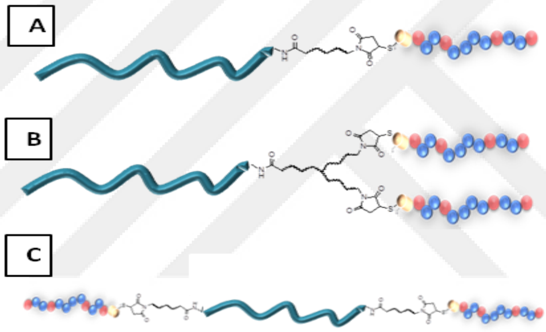

Figure 3.2 Schematic representation of the polymer-peptide conjugates. (a) PEG-pep, (b) PEG-(pep)$_2$, (c) pep-PEG-pep.

3.5 Purification of Polymer-peptide Conjugates

The synthesized conjugates were dissolved in 50% ACN. By using HPLC (260 Infinity Quaternary LC systems, Agilent Technologies) with the help of C-18 column (RPC 250x10 mm ID hydrophobic 6µm, Agilent VariTide), polymer-peptide conjugates were purified. UV absorption at 214 nm, 193 nm, 254 nm, and 280 nm was used to detect peaks. At 2 mL/min flow rate, ddH$_2$O (include 0.05% TFA) and ACN (include 0.025% TFA) were used as mobile phases A and B for the system, respectively.

3.6 Concentration Calculation of the Peptides and Conjugates

The synthesized peptides and conjugates concentrations were measured by UV-vis spectrophotometer (NanoDrop™ One/OneC Microvolume, Thermo Scientific). For measurement, a standard curve was drawn using the peptide standards included in the kit (Pierce™ quantitative fluorometric peptide assay, Thermo Scientific™). The final concentration of standard A was 841 µM and was prepared as a stock standard solution. Peptides absorb in the UV region between 190–220 nm and are used for concentration measurement.

All measurements of standards and samples were made with three replicates, based on 214 nm, which was also purified in HPLC. To calculate the concentration of the peptides and conjugates from µM to mg/mL the following equation was used:

$$\text{Concentration (mg/mL)} = \frac{\text{Abs. (214 nm)}}{\text{Slope of standart curve}} \times \frac{\text{Mw of Peptide (Da)}}{10^6} \quad \text{(eq.1)}$$

3.7 Characterization of Polymer-peptide Conjugates

3.7.1 HPLC analysis

Synthesized polymer-peptide conjugates were dissolved in 50% acetonitrile (ACN). By using HPLC (260 Infinity Quaternary LC systems, Agilent Technologies) with the C-18 column (RPC 250 x 10 mm ID hydrophobic 6 µm, Agilent VariTide), polymer-peptide conjugates were analyzed. UV absorption at 214 nm, 193 nm, 254 nm, and 280 nm was used to detect peaks. At 2 mL/min flow rate, ddH_2O (include 0.05% TFA) and ACN (include 0.025% TFA) were used as mobile phases A and B for the system, respectively.

Table 3.9 prep RP-HPLC method used for analysis of PEG-pep and PEG-(pep)$_2$ conjugates.

Method	
Time (min)	B solution (%)
0–20	1–15%
20–30	15–100%

Table 3.10 prep RP-HPLC method used for analysis of pep-PEG-pep conjugate.

Method	
Time (min)	B solution (%)
0–1	0%
1–31	0–100%
31–33	100%

3.7.2 FT-IR analysis

Chemical characterization of the peptides and conjugates were measured by fourier transform infrared spectroscopy (FT-IR, Nicolet iS10 Thermo Fisher) to determine the presence of the bonds. Dry form samples were placed directly contact with the attenuated total reflection (ATR) sampling accessory. Air was measured as a background and then samples were analyzed. Each sample spectrum was measured from 400 cm^{-1} to 4000 cm^{-1} wavenumber with 32 scans at room temperature.

3.7.3 ^{1}H NMR analysis

The chemical structure of the purified peptides and conjugates were characterized using proton nuclear resonance (^{1}H NMR) on a 400 MHz Bruker NMR spectrometer in DMSO-d_6.

3.8 *In Vitro* Evaluation of Polymer-Peptide Conjugates

3.8.1 Antimicrobial activity

Escherichia coli (*E. coli* ATCC® 25922), *Staphylococcus aureus* (*S. aureus* ATCC® 25923), *Candida albicans* (*C. albicans* ATCC® 10231), *Pseudomonas aeruginosa* (*P. aeruginosa* ATCC® 27853), vancomycin-resistant *Enteroccus faecium* (VRE-*faecium*, ATCC®), and methicillin-resistant *S. aureus* (MRSA, ATCC®) were incubated in Mueller-Hinton Agar (MHA) at 37°C, overnight. Then, a colony was selected and transferred to Mueller-Hinton Broth (MHB). To each bacterial solution in the MHB were adjusted to 0,5 McFarland (8 x 10^7 cell/mL), OD600 value between 0,08–0,1 using UV-vis Spectrophotometer. 0,5 McFarland bacteria cultures were diluted to 1:100 ratio in MHB. Serial dilutions of peptides and conjugates (1024–0,5 µg/mL) were prepared in MHB with a total volume of 95 µL in a round-bottom 96-well plate. 5 µl of the prepared bacterial suspensions were added into sample dilutions in each well prepared. Naked AMP (TN6) and Ampicillin (GeneMark) were used as a control. Also, %50 ACN was used as a negative control and bacterial solutions were used directly as a positive control. All round-bottom 96-well plates were incubated at 37°C, overnight and all samples were prepared in triplicate. Then, samples were measured at 600 nm using a microplate reader (Gen5 Synergy HT BioTek).

3.8.2 Cytotoxicity assay

Human epidermal keratinocyte (HaCaT, ATCC PCS-200-011) and mouse fibroblast (3T3, ATCC CRL-1658) were used as cell lines. Dulbecco's Modified Eagle Medium (DMEM) has been completed with 1% Pen/Strep antibiotics (100 U/mL of penicillin and 100 µg/mL of streptomycin) and 10% fetal bovine serum (FBS). Cell lines were incubated with complete DMEM at 37°C, 5% CO_2 condition, and 90% humidity until 80-100% confluency was reached. Medium was discarded from cell flask, cells were washed with 1X phosphate buffer saline (PBS), trypsinized with 0,25% trypsin-EDTA solution, and incubated at 37°C for 5 min. After, trypsin was deactivated with DMEM at room temperature, the detached cells were collected in falcon and centrifuged at 500 g for 5 min. The supernatant was discarded, and the cell pellet was resuspended with complete DMEM. 10 μL of cell solution was stained with 1:1 ratio of trypan blue and counted with a thoma hemocytometer. To count the cells the following equation was used:

$$\text{Cells (cell/mL)} = \text{Mean of cells x Dilution factor (DF) x Volume of Thoma } (10^4) \tag{eq.2}$$

After cell counting, for cytotoxity test (MTT, Cell Proliferation Kit, Roche), 5 x 10^4 cells/well in 100 μL were placed in flat-bottom 96-well plate and incubated in 5% CO_2 at 37°C for 24 h to attach the cells. After, the medium on the cells was discarded. Serial dilutions of peptides and conjugates (1024–0,5 μg/mL) were prepared in DMEM with a total volume of 100 μL. Magainin II (Mag2) which is a non-toxic antimicrobial peptide found in nature, was used as a positive control for the assay. All samples were prepared in triplicate. Serial dilutions of peptides, control group, and conjugates were added to the cell-seeded plates and were incubated in 5% CO_2 at 37°C for 24 h. According to the MTT kit, 10 μL of MTT labeling reagent was added to the top of samples in each well round bottom 96-well plate and incubated in 5% CO_2 at 37°C. After 4 h of incubation, 100 μL of kit solubilization solution (10% SDS in 0,01 M HCl) was added to each well and incubated in 5% CO_2 at 37°C. After 24 h, the purple formazan salt formed was measured at 550 nm and 690 nm by using a microplate reader.

3.8.3 Hemolytic activity (HC50)

The hemolytic activity test measures the percentage of erythrocytes lysed depending on the dose due to the treatment of the sample to be used with blood cells. 300 μL of fresh human blood was suspended with using 20 mL of sterile Tris-saline (150 mM NaCl, 10 mM Tris, pH 7,2) solution then centrifuged at 1500 rpm for 5 min. The supernatant was discarded, and the pellet was resuspended with 20 mL of Tris-saline buffer, three times. At the final step, pellet was dissolved with 100 mL of Tris-saline, and 100 μL blood mix was added into each well of 96-well plate. Serial dilutions of peptides and conjugates (1024–0,5 μg/mL) were prepared in sterile Tris-saline with a total volume of 100 μL. 100 μL of each sample was added on top of blood mix. 20% DMSO and Triton X-100 were mixed in a 1:1 ratio to use as a positive control. Also, sterile Tris-salin was used as a negative control. The samples were kept on separate round-bottom 96-well plates at 37°C for 30 min and 1 hour, respectively to evaluate two different conditions. All samples were prepared in triplicate. After incubations, the 96-well plates were centrifuged at 1500 rpm for 10 min. The supernatants were transferred into a new 96-well plate for measurement at 414 nm by using a microplate reader. The % lysis of the peptide and conjugates were calculated using the following equation (120):

$$\text{Hemolysis (\%)} = \frac{\text{Sample (414 nm)} - \text{Negative control (414 nm)}}{\text{Positive control (414 nm)} - \text{Negative control (414 nm)}} \times 100 \qquad \text{(eq.3)}$$

3.8.4 Cell-associated hemolytic activity assay

Cell-associated hemolytic activity assay shows the percentage of erythrocytes that are hemolyzed during the infection of the blood with bacteria, depending on the drug dose. 300 μL of fresh human blood was suspended with using 20 mL of sterile Tris-saline (150 mM NaCl, 10 mM Tris, pH 7,2) solution then centrifuged at 1500 rpm for 5 min. The supernatant was discarded, and the pellet was resuspended with 20 mL of Tris-saline solution, three times. As a final step, pellet was dissolved with 100 mL of Tris-saline and 100 μL blood mix was added into each well of 96-well plate.

S.aureus 25923 was incubated in Mueller-Hilton Agar (MHA) at 37°C, overnight. Then, a colony was selected and transferred to MHB. To each bacterial solution in the MHB were measured at 600 nm by UV-vis spectrophotometer and adjusted to 1,5 x 10^6 CFU/mL. 5 μL bacterial solution was added to the 96-well plate containing the blood mixture diluted with Tris-saline.

Serial dilutions of the peptides and conjugates (1024–0,5 μg/mL) were prepared in sterile Tris-saline with a total volume of 100 μL. 100 μL of each sample was added on top of bacteria-blood mix. 20% DMSO and Triton X-100 were mixed in a 1:1 ratio to use as a positive control. Sterile Tris-salin was used as a negative control. Also, blood mixture and bacteria-blood mixture were used as controls. All 96-well plates were incubated at 37°C for 1 h and all samples were prepared in triplicate. After incubations, the 96-well plates were centrifuged at 1500 rpm for 10 min. The supernatants were transferred into a new 96-well plate for measurement at 414 nm by using a microplate reader. The % lysis of the peptide and conjugates were calculated by using the following equation:

$$\text{Hemolysis (\%)} = \frac{\text{Sample (414 nm)} - \text{Negative control (414 nm)}}{\text{Positive control (414 nm)} - \text{Negative control (414 nm)}} \times 100 \qquad \text{(eq.4)}$$

3.8.5 Stability towards plasma proteases

To evaluate the impact of human plasma proteases on the antimicrobial activities of the peptide and conjugates, the MIC values of the samples after various incubation time points with human plasma were determined. To separate human plasma, EDTA-treated fresh human blood was centrifuged at 1500 rpm for 5 min and the supernatant was collected. The peptide and conjugates were mixed with human plasma to a final concentration of 0,1 mg/mL (1,7 µL 2048 µg/mL sample completed with plasma) and incubated at 37°C, 1500 rpm in shaker. Aliquots (35 µL) were removed after 0 h, 6 h, and 24 h and stored at –20°C. 5 µL protease inhibitor (Roche, cOmplete™ Mini protease inhibitor cocktail) was added onto 35 µL aliquots.

S.aureus 25923 was incubated in MHA at 37°C, overnight. Then, a colony was selected and transferred to MHB. The bacterial solution in the MHB was adjusted to 0,5 McFarland (1,0 x 10^8 CFU/mL) and was diluted to a 1:200 ratio in MHB. Serial dilutions of aliquots (147–0,07 µg/mL) were prepared in MHB with a total volume of 40 µL in a round-bottom 96-well plate. 5 µl of the prepared bacterial suspension were added into sample dilutions in each well prepared. and were incubated at 37°C, overnight. Then, 96-well plates were measured at 600 nm by using a microplate reader (121).

3.8.6 Sample preparation for electron microscopy

For scanning electron microscope (SEM) and transmission electron microscope (TEM) evaluation, three different samples (Cpep-PEG-Cpep, pepC-PEG-pepC conjugate and TN6) and *E. coli* ATCC 25922 as a control were studied. The bacteria in the MHB were adjusted to OD600 value between 1,0 using UV-vis spectrophotometer.

Cpep-PEG-Cpep, pepC-PEG-pepC, and TN6 peptide concentrations were adjusted 1 mg/mL, 3 mg/mL, and 138 μg/mL, respectively. 100 μL of each sample and 500 μL of the bacterial solution were mixed and incubated at 37°C for 4 h (122).

3.8.7 SEM

After 4 h, 10 μL of each sample solution was taken and dropped onto the dialysis membrane (Spectra/Por® molecular porous membrane tubing, 0,45 μm pore size) for preparation of SEM samples. All remaining sample solutions were used for the preparation of TEM samples.

Bacterial samples were fixed in 2,5% glutaraldehyde fixative in PBS buffer (pH 7.2) for 4 h. The samples were washed with PBS buffer for 12 h. After, post-fixation was performed with 1% osmium tetroxide for 1 h and washed again with PBS for 15 min. The samples were dehydrated by passing through alcohol series (50%, 70%, 90%, 96%, and 100%) for various time points (5 min, 10 min, 10 min, 10 min, 15 min (two times), respectively). Following dehydration, the samples were rinsed with 2/1, 1/1, 1/2 alcohol /amyl acetate, and pure amyl acetate series for 15 min to each step. The samples were dried and taken onto grids. Then, they were coated with gold after drying in the critical point dryer and examined with SEM (Thermo Scientific-Quattro SEM).

3.8.8 TEM

The remaining sample solution in Eppendorf was centrifuged at 10.000 rpm for 5 min. The supernatant was discarded, and pellets were fixed in 2,5% glutaraldehyde fixative in PBS buffer (pH 7,2) for 4–12 hours. The pellets were washed with PBS for 5 min and removed. Pellets were treated with 1% osmium tetroxide for 1 h. After treatment, osmium solution was removed and centrifuged at 10.000 rpm for 5 min. After discarding supernatant, the pellets were embedded in agar. The samples were washed with 50%, 70%, 90%, 96%, and 100% of alcohol series and pure propylene for different times (5 min, 10 min, 10 min, 10 min, 15 min (two times), 15 min (two times), respectively). Then, 1/1 propylene-Epon was added to samples and the samples in the Eppendorf were rotated with a 360°C tube rotator at room temperature, overnight. The agar samples were embedded into pure Epon 812 (Sigma-Aldrich). It was dried under vacuum for 1 h and outside for 2 h to get rid of air bubbles. Before taking thin sections (around 60 nm thickness) with Ultramicrotome (Leica EM UC7) from agar blocks, the samples were polymerized overnight at 60°C in an oven. The sections were placed on TEM grids and contrasted. For the contrast step, 1 mL 3% uranyl acetate solution (Sigma-Aldrich) was centrifuged at 14.000 rpm, 4°C for 15 min, and the supernatant was dropped onto the matte surface of the grid for 25 min. Then, each grid was rinsed with dist. water and examined by TEM (Thermo Scientific-Talos L120C).

3.9 Statistics

All given data were analyzed by GraphPad Prism 9. The results were shown as mean ± SD. Statistical analyses between concentration and groups were expressed using two-way analysis of variance (ANOVA) with mixed-effects analysis. A p-value less than 0,05 was considered statistically significant.

4. RESULTS

4.1 Purification of the Peptides and Conjugates

a)

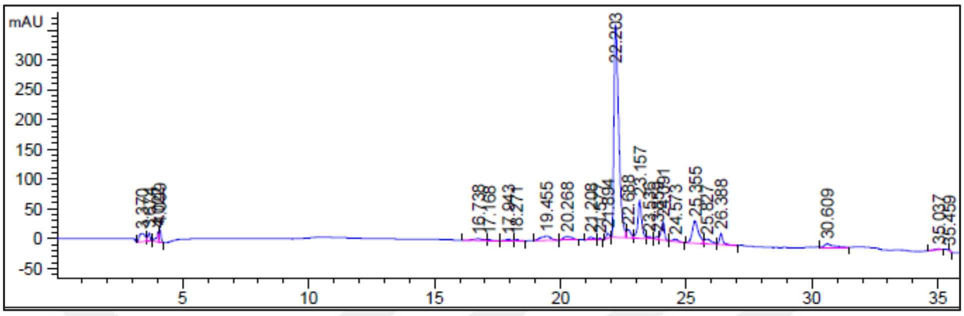

b)

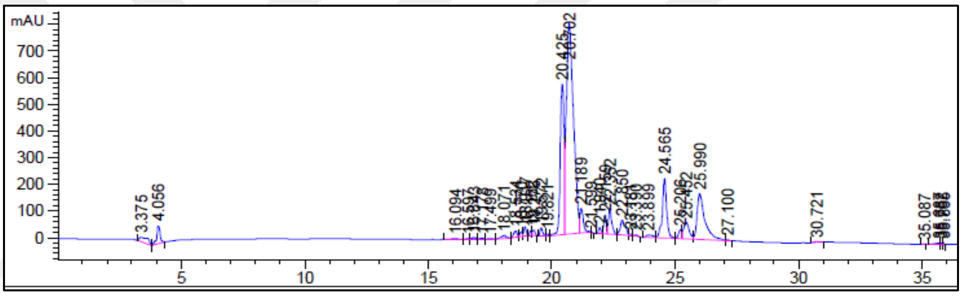

c)

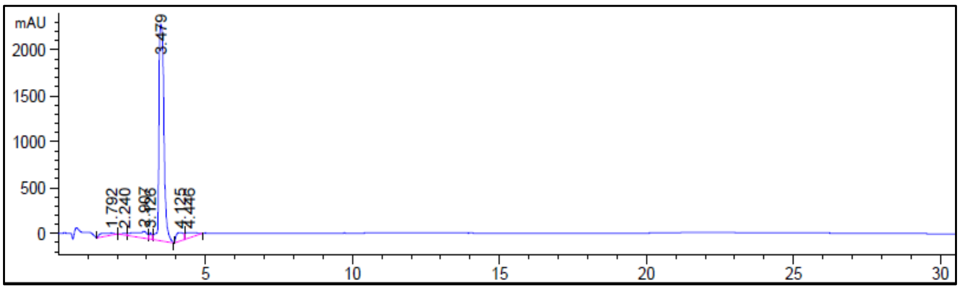

d)

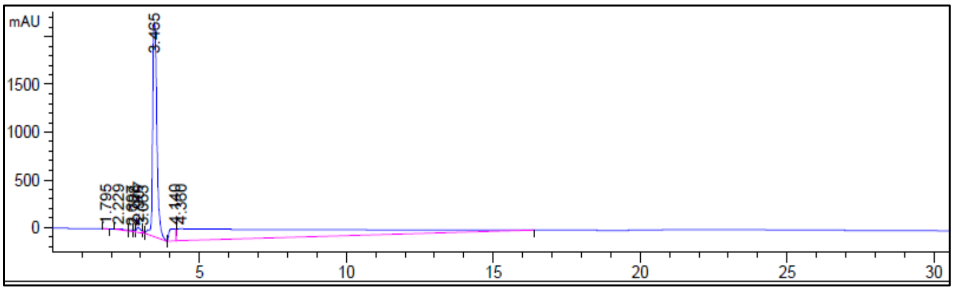

e)

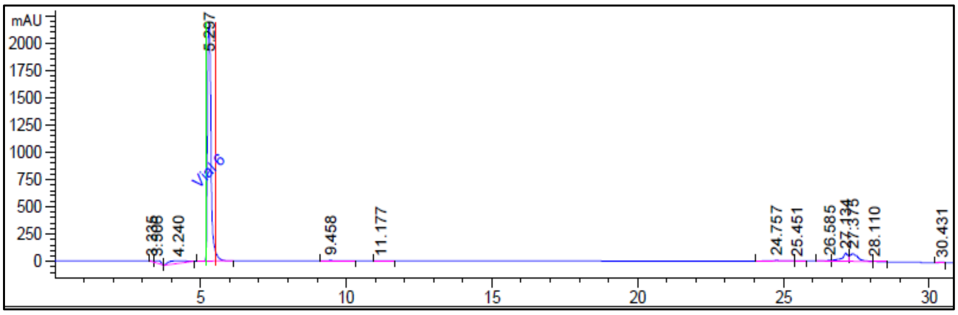

f)

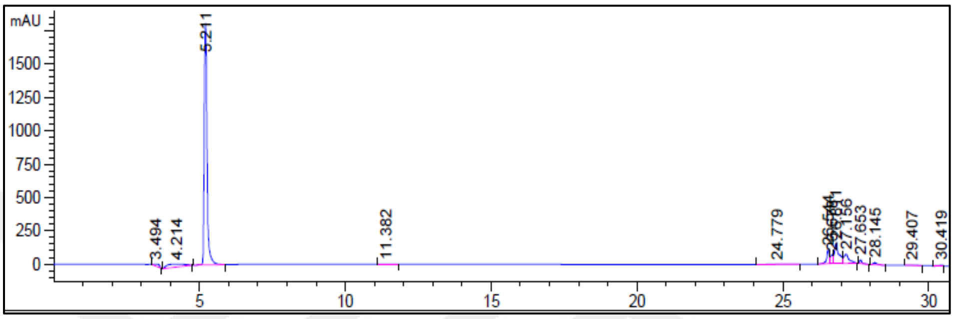

g)

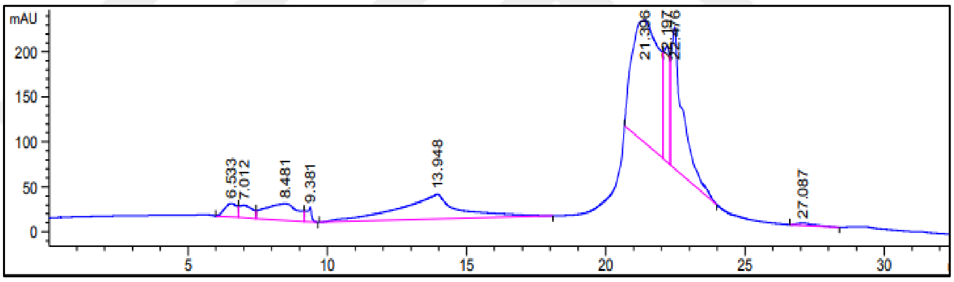

h)

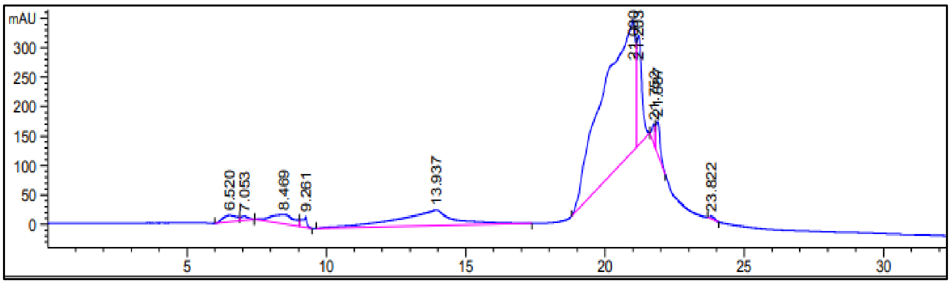

Figure 4.1 HPLC chromatograms of peptides and polymer-peptide conjugates. a) C-TN6 peptide, b) TN6-C peptide, c) PEG-Cpep, d) PEG-pepC, e) PEG-$(Cpep)_2$, f) PEG-$(pepC)_2$, g) Cpep-PEG-Cpep, h) pepC-PEG-pepC.

Since peptide and peptide-linked conjugates were observed at 214 nm, peaks at 214 nm were examined in all HPLC results. After synthesis of the modified peptides, the method given in Table 3.3 was applied using prep-HPLC for purification. During purification, the signal from 22–23. min was collected for the C-TN6 peptide (a) in Figure 4.1. According to the method, signal corresponds to 47–49% ACN. TN6-C peptide (b) was also purified using the same method, and the peptide signal was observed between 20–22. min, which corresponds 42–45% ACN.

The method in Table 3.9 was used for both PEG-pep and PEG-$(pep)_2$ designs. PEG-Cpep (c) and PEG-pepC (d) peaks were collected at 3–4. min, which corresponds 2,1–2,8% ACN ratio in both. For PEG-$(Cpep)_2$ (e) and PEG-$(pepC)_2$ (f), the peaks at 5–6. min corresponding to 3,5–4,2 %ACN ratio were collected. The method in Table 3.10 was applied for Cpep-PEG-Cpep (g) and pepC-PEG-pepC (h) conjugates. According to this method, conjugates were collected at 21 and 22 min, corresponding to 67–70% ACN.

4.2 Analysis of the Peptides and Conjugates

4.2.1 LC/MSMS

Table 4.1 Mass to charge ratio of the synthesized peptides.

m	z	m/z
1537	1	1537
1537	2	768.5
1537	3	512.3
1537	4	384.3
1537	5	307.4

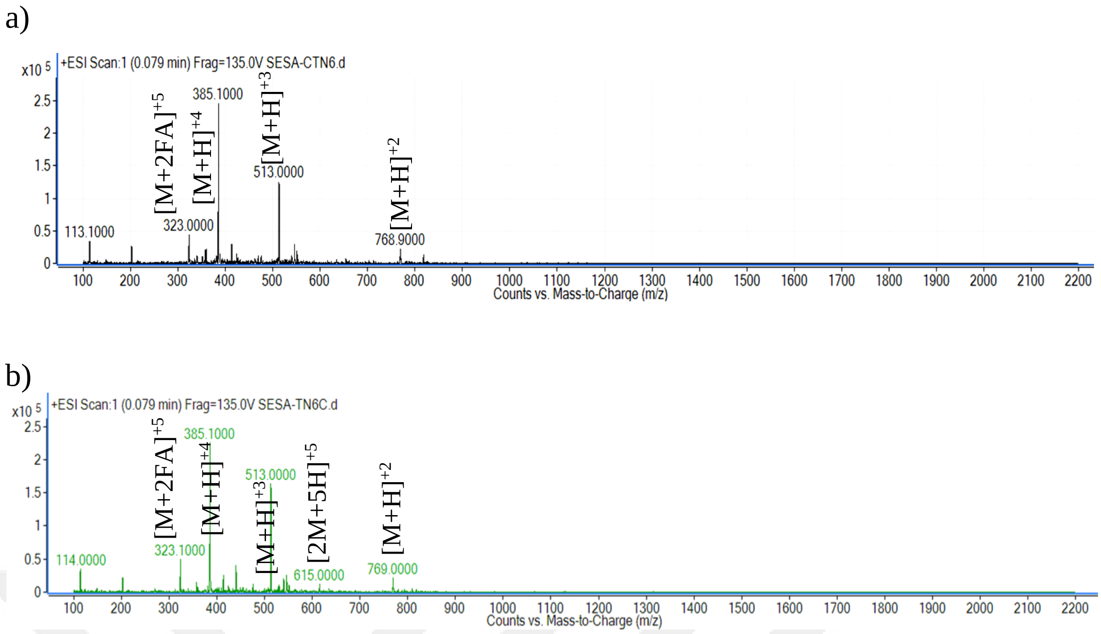

Figure 4.2 LC/MSMS analysis of the peptides. a) C-TN6 peptide, b) TN6-C peptide.

Mass/charge (m/z) ratios of C-TN6 and TN6-C peptides were calculated (Table 4.1). According to the calculation, peptide fragments expected to be observed in the LC/MSMS spectrum due to ionization were obtained. Figure 4.2 shows the LCMSMS spectra of the C-TN6 (a) and TN6-C (b) peptides. The notations on the fragments show whether the peaks obtained from the purified peptide molecules are at the desired molecular weight.

4.2.2 FT-IR

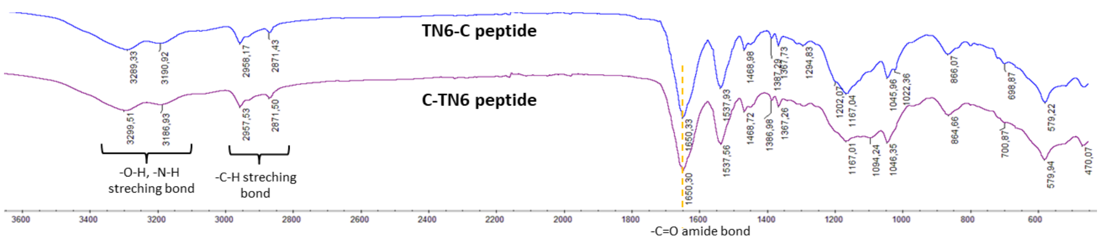

Figure 4.3 FT-IR analysis of the TN6-C and C-TN6 peptides.

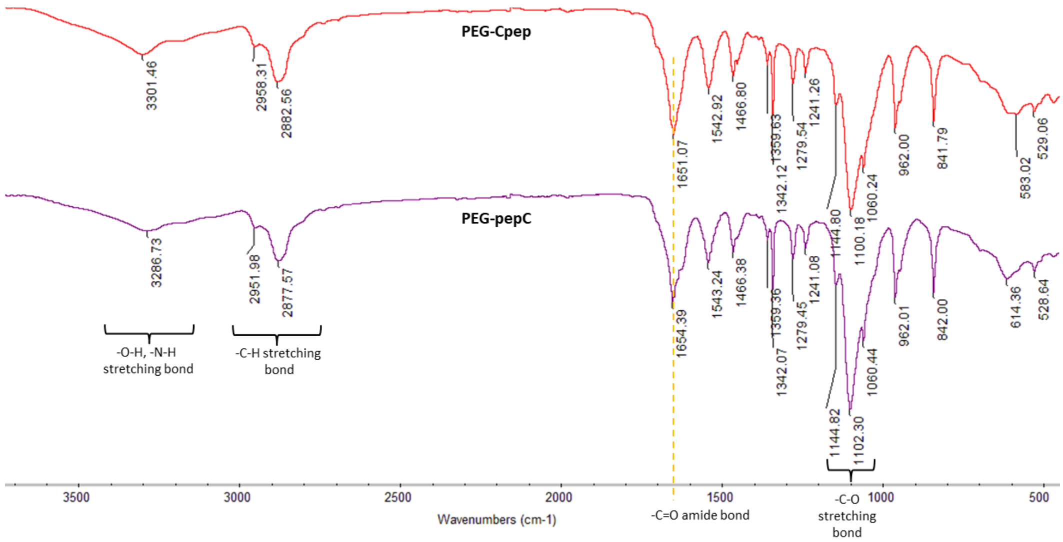

Figure 4.4 FT-IR analysis of the PEG-Cpep and PEG-pepC conjugates.

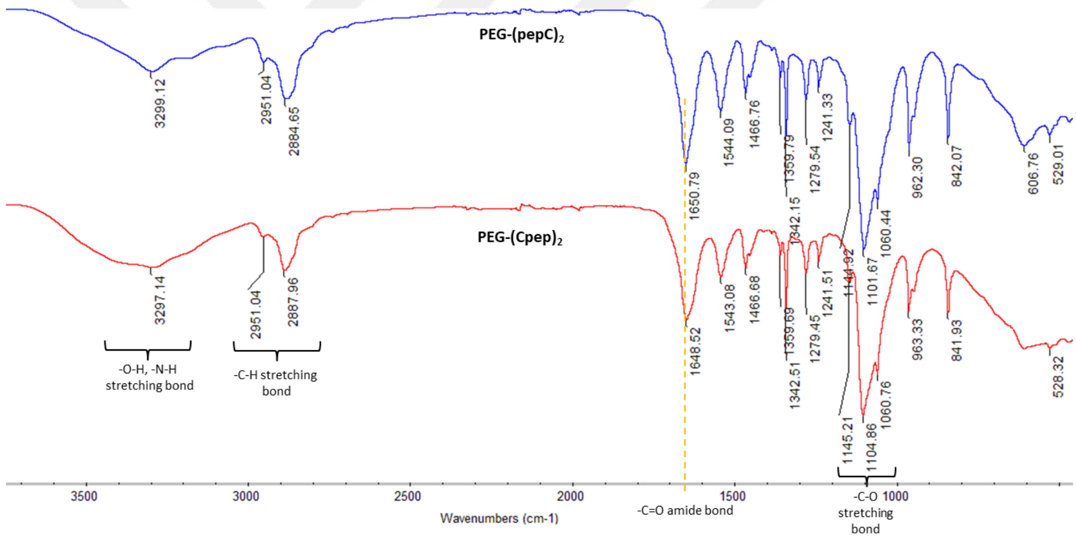

Figure 4.5 FT-IR analysis of the PEG-$(pepC)_2$ and PEG-$(Cpep)_2$ conjugates.

FT-IR analysis of the peptides (Figure 4.3) and conjugates (Figure 4.4–4.6) indicated the existence of the bonds by the modified peptides and PEG polymer. C-O stretching bond (1060–1145 cm^{-1}) coming from PEG polymer was shown in all nanostructures. C=O amide bond (~1650 cm^{-1}), C-H stretching bond (2870–2960 cm^{-1}), and N-H and O-H stretching bonds (3302–3180 cm^{-1}) were demonstrated for the modified peptides and all nanostructures.

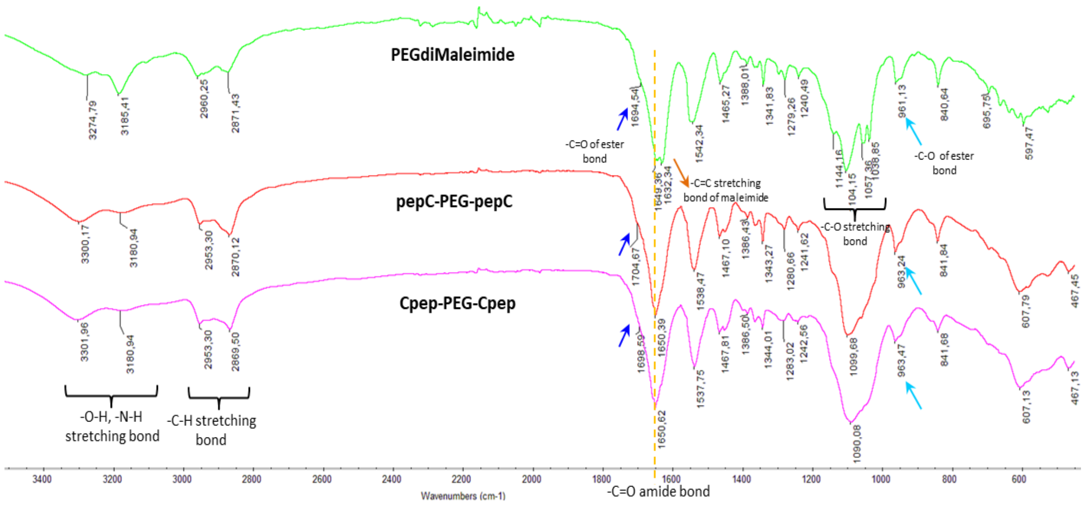

Figure 4.6 FT-IR analysis of the PEGdiMaleimide molecule, pepC-PEG-pepC, and Cpep-PEG-Cpep conjugates.

The PEGdiMal molecule, intermediate molecule for pep-PEG-pep synthesis, has a sharp C=C stretching bond (1632 cm^{-1}) in the maleimide group (Figure 4.6). The loss of the C=C stretching bond shows that the peptide molecules were successfully attached from both sides of the PEG polymer for the pep-PEG-pep design. Furthermore, the C-O bond (~960 cm^{-1}) and C=O bond (1695–1705cm^{-1}) of the ester group of the linker in this conjugate are clearly seen.

4.2.3 ^{1}H NMR

The chemical structures of the conjugates were investigated by ^{1}H NMR spectroscopy in d_6-DMSO, which revealed both peptide-specific protons and PEG polymer components.

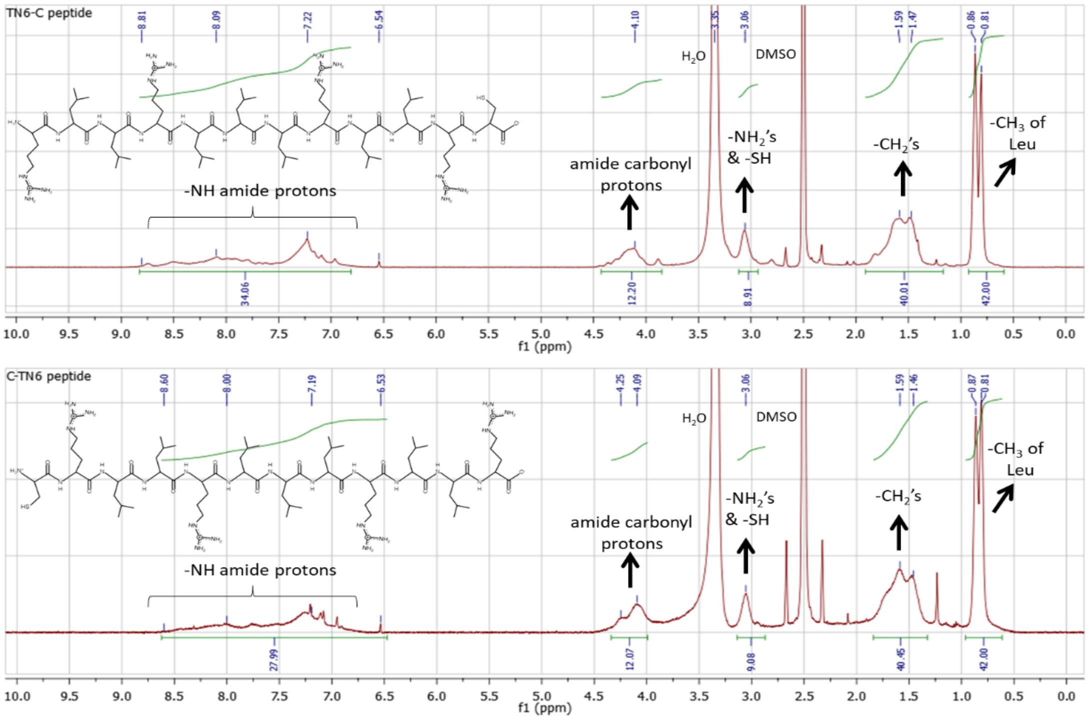

Figure 4.7 ^{1}H NMR analysis of the TN6-C and C-TN6 peptides.

Figure 4.7 shows the proton spectra of the modified TN6 peptides. Because the sequences of the two peptide molecules are similar, proton NMR results were almost identical. So, the conjugates included C-TN6, or TN6-C peptides were predicted to emit similar protons in their spectrum. A comparison of the peptide spectra shows the existence of both labile protons as a broad multiplet at 6,9-8,7 ppm, amide carbonyl protons at 4,10 ppm, and a doublet at 0,84 ppm (coupling constant *J* = 20) from isopropyl groups of the leucine (Leu). In addition, DMSO protons were seen clearly at 2,5 ppm with satellites on both sides.

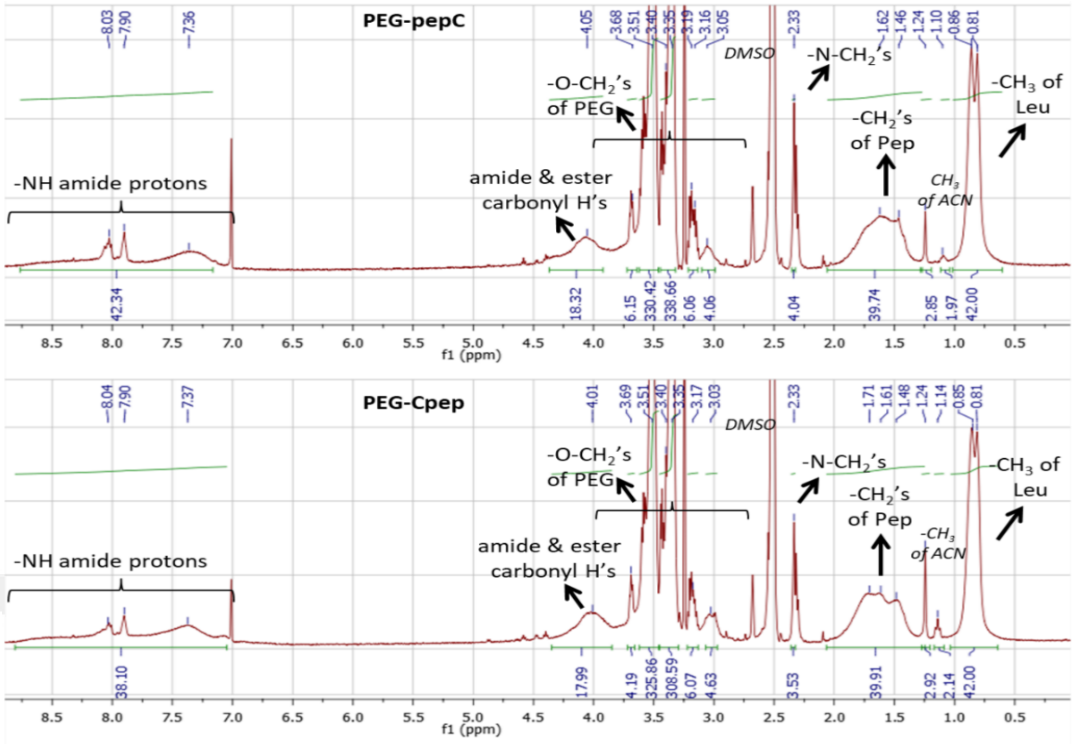

Figure 4.8 ^{1}H NMR analysis of the PEG-Cpep and PEG-pepC conjugates.

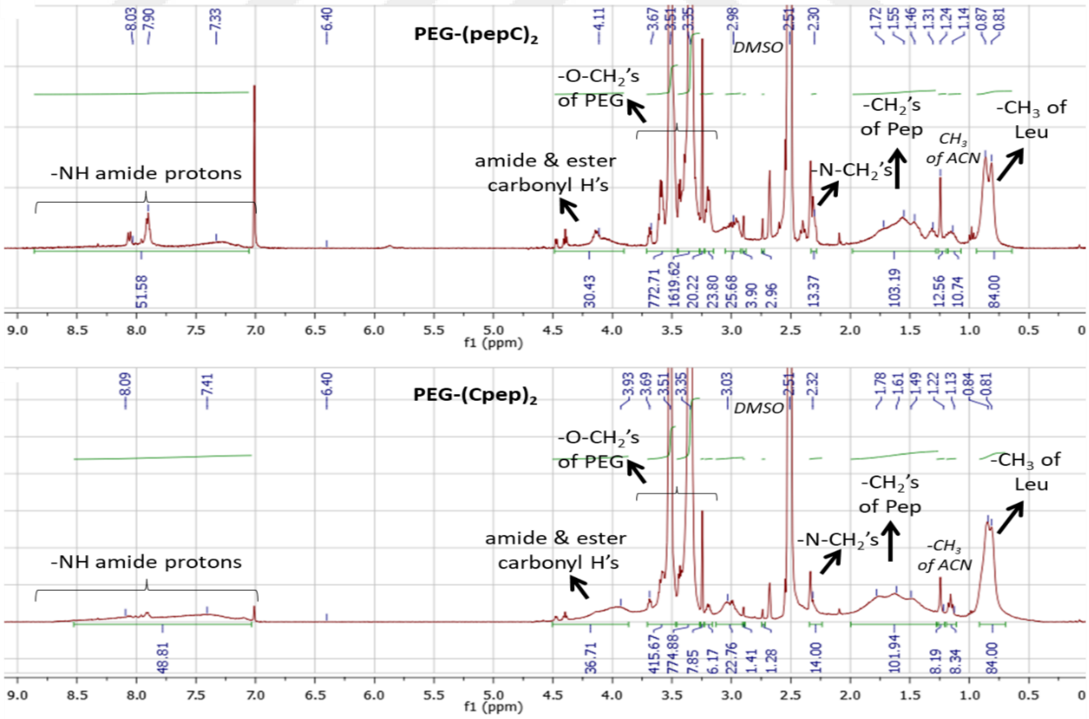

Figure 4.9 ^{1}H NMR analysis of the PEG-(pepC)$_2$ and PEG-(Cpep)$_2$.

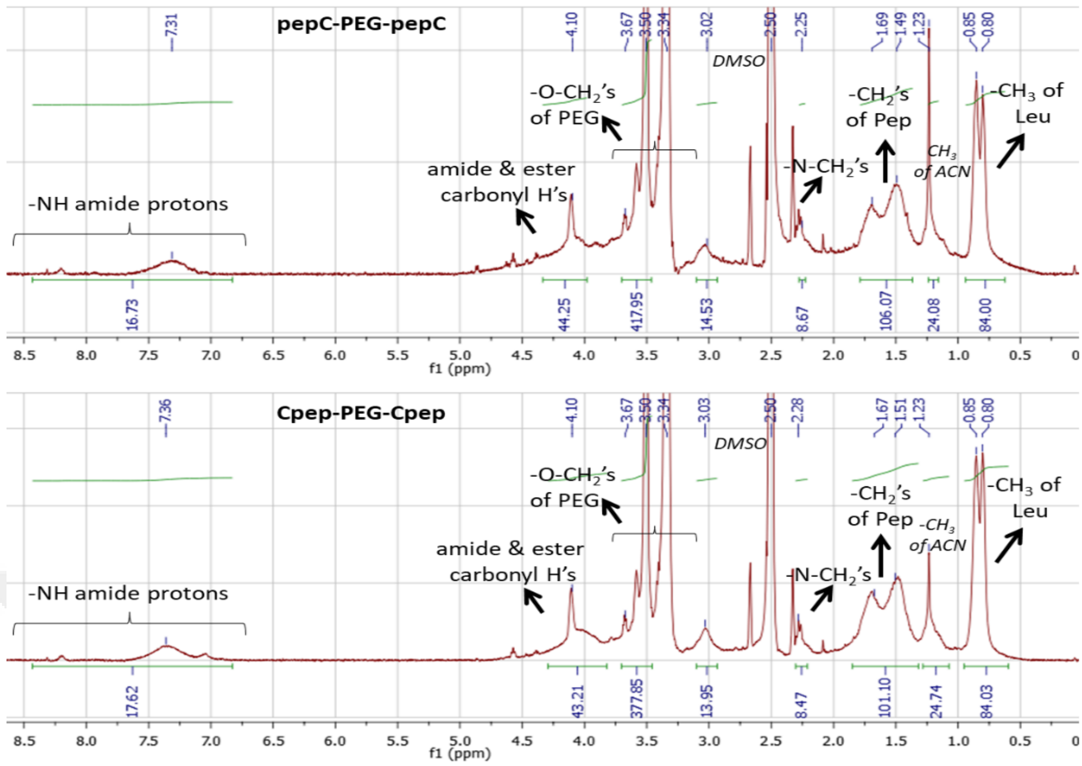

Figure 4.10 ^{1}H NMR analysis of the pepC-PEG-pepC and Cpep-PEG-Cpep.

The high-intensity triplet peak, corresponding to 3,50 ppm in the NMR spectra of all conjugates, indicates –O-CH_2 protons from the PEG polymer (Figure 4.8–4.10). In addition, the peptide peaks seen in Figure 4.7 are also seen in all conjugates.

When conjugates containing a single peptide (Figure 4.8) were compared with conjugates containing two peptides (Figure 4.9–4.10), the integration of isopropyl -CH_3 protons and amide carbonyl protons originating from the peptide was nearly doubled in PEG-(pep)$_2$ and pep-PEG-pep conjugates. Thanks to the comparison, we can confirm the chemical structure of conjugates containing one peptide or two peptides. Moreover, when the difference between the NMR spectra of PEG-(pep)$_2$ (Figure 4.9) and pep-PEG-pep (Figure 4.10) conjugates is analyzed, extra ester carbonyl protons are seen at 3,67–3,25 ppm in pep-PEG-pep conjugates. This change originated due to the linker molecule in the pep-PEG-pep conjugate.

4.3 *In vitro* Evaluation of Polymer-peptide Conjugates

4.3.1 Minimal inhibitory concentration (MIC)

The peptide and conjugates were evaluated against six different pathogenic or resistant microorganisms. Also, ampicillin was used as a positive control group. For all replicates, the identical results were seen.

Table 4.2 MICs for the peptides and conjugates against pathogenic and resistant microorganisms.

Microorganism	Minimum Inhibitory Concentration (µg/mL)							
	PEG-Cpep	PEG-pepC	PEG-(Cpep)$_2$	PEG-(pepC)$_2$	Cpep-PEG-Cpep	pepC-PEG-pepC	TN6	ampicillin
S. aureus 25923	64	16	128	64	4	32	1	8
E. coli 25922	64	16	128	128	4	64	1	32
P. aeruginosa 27853	128	128	256	256	32	128	4	256
C. albicans 10231	32	32	128	64	8	16	1	16
MRSA	84	21	120	105	12	25	0,78	32
VRE-faecium	84	21	120	52	12	25	1,56	16

None of the components of the conjugate (PEG polymers and linkers) except the peptide showed antimicrobial activity when tested alone, while the naked peptide (TN6) demonstrated the highest antimicrobial activity. Evaluating the MIC, in all tested microorganisms, the Cpep-PEG-Cpep conjugate had the highest antifungal/antibacterial activity compared to ampicillin antibiotic and other conjugates, while the PEG-(Cpep)$_2$ had the lowest activity. With the exception of *Candida albicans*, the PEG-pepC had the second-best antibacterial activity. In addition, the pepC-PEG-pepC had the second-best antibacterial activity against *C. albicans* (Table 4.2).

4.3.2 Cytotoxicity assay

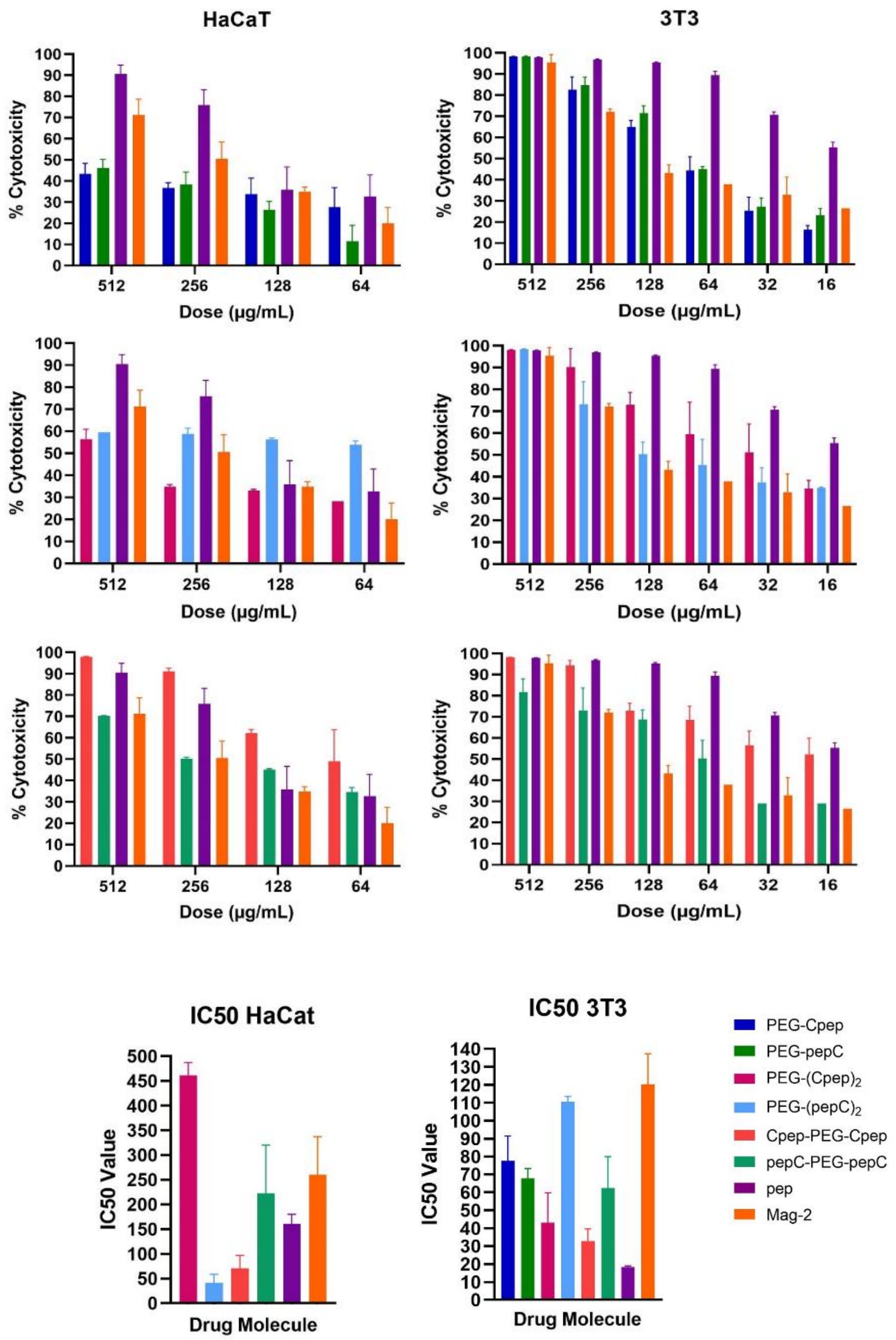

Figure 4.11 Dose-dependent cytotoxicity of all conjugates on HaCaT and 3T3 cells for 24 h.

Cytotoxicity data were shown as mean ± SD and analysis with two-way ANOVA. P values of each graph were evaluated statistically significant ($p < 0.0001$) (Figure 4.11). The MTT test was used to assess the cytotoxicity for all conjugates. The cytotoxicity was evaluated as dose dependent for HaCaT and 3T3 cell lines. Cell cytotoxicity rose with increasing peptide and conjugate doses.

The inhibitory concentration (IC50) values of the HaCaT cells were >512 µg/mL, >512 µg/mL, 461,44 µg/mL, 41,36 µg/mL, 70,61 µg/mL, 222,27 µg/mL, 160,57 µg/mL, and 260,22 µg/mL for PEG-Cpep, PEG-pepC, PEG-(Cpep)$_2$, PEG-(pepC)$_2$, Cpep-PEG-Cpep, pepC-PEG-pepC, pep, and Mag-2, respectively.

According to the IC50 values in HaCaT cells, PEG-(Cpep)$_2$ had the least cytotoxicity, whereas PEG-(pepC)$_2$ has the most. Even at the highest concentration (512 µg/mL) tested, no IC50 dosage was identified in PEG-pep conjugates. Meanwhile, pepC-PEG-pepC conjugate has a significantly lower cytotoxic effect than Cpep-PEG-Cpep conjugate. PEG-(pepC)$_2$ and Cpep-PEG-Cpep conjugates were shown to be more toxic than the peptide itself.

In the 3T3 cell line, IC50 values were 77,70 µg/mL, 67,70 µg/mL, 43,02 µg/mL, 110,51 µg/mL, 32,82 µg/mL, 62,35 µg/mL, 18,43 µg/mL, and 120,35 µg/mL for PEG-Cpep, PEG-pepC, PEG-(Cpep)$_2$, PEG-(pepC)$_2$, Cpep-PEG-Cpep, pepC-PEG-pepC, pep, and Mag-2, respectively.

Based on IC50 values for 3T3 cells, PEG-(pepC)$_2$ was the least cytotoxic conjugate, whereas Cpep-PEG-Cpep was the most cytotoxic. In comparison to all samples, the peptide was the most toxic chemical at all doses.

4.3.3 Hemolytic activity

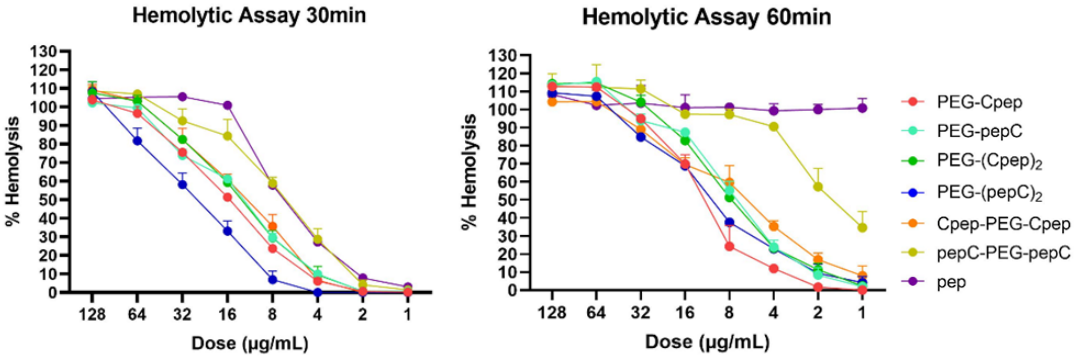

Figure 4.12 Dose-dependent hemotoxic effect of all conjugates for 30 min and 60 min.

Hemolytic activity data were indicated as mean ± SD and analysis with two-way ANOVA. P values of each graph were evaluated statistically significant ($p < 0.0001$). Figure 4.12 shows the dose-dependent percentages of hemolysis at different periods for all conjugates. At all periods, the TN6 peptide had the highest hemolytic activity. After 30 minutes of incubation, all TN6 peptide dosages tested were substantially over the toxic dose (HC50), which damaged 50% of the erythrocytes.

For the 30 min hemolytic assay, PEG-$(pepC)_2$ had the lowest hemolysis rate at all concentrations among the conjugates treated with fresh human erythrocytes, while pepC-PEG-pepC had the highest hemolysis rate. The TN6 peptide's and all conjugates' hemolytic activity increased after 60 min treatment compared to 30 min. PEG-Cpep had the least increment in hemolytic activity.

4.3.4 Cell-associated hemolytic activity assay

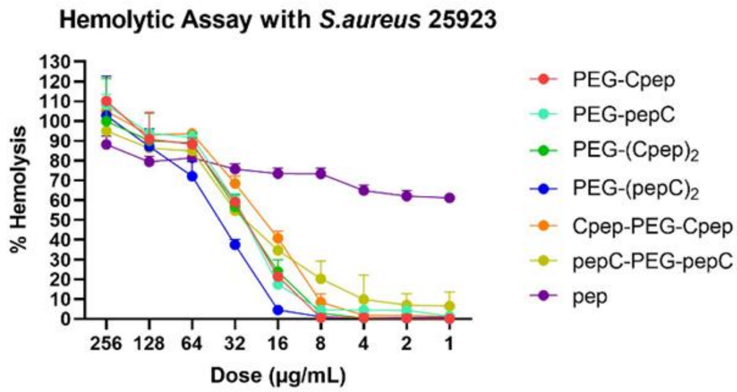

Figure 4.13 Dose-dependent and *S. aureus*-associated hemotoxic effect of all conjugates for 60 min.

Cell-associated hemolytic activity data were shown as mean ± SD and analysis with two-way ANOVA. P value of graph was evaluated statistically significant ($p < 0.0001$). The *S. aureus*-associated hemolytic assay demonstrated that PEG-$(pepC)_2$ had the lowest hemolytic activity during the 60-minute treatment, whereas Cpep-PEG-Cpep had the highest. When compared to a 60-minute treatment without bacteria, the *S. aureus*-associated hemolytic activity of pepC-PEG-pepC decreased 15-fold from 2,36 g/mL to 31,12 g/mL. Furthermore, the HC50 doses of PEG-pepC, Cpep-PEG-Cpep, and PEG-$(Cpep)_2$ decreased around four times in this comparison. In hemolysis data with or without bacteria in 60 minutes, the TN6 showed hemolytic activity in all concentrations.

4.3.5 Biological protease assay

Table 4.3 Antimicrobial activity after plasma plasma proteases for TN6 peptide and pep-PEG-pep conjugates.

Hours (h)	Antimicrobial Activity After Plasma Proteases (µg/mL)			
	pep	Cpep-PEG-Cpep	pepC-PEG-pepC	blood plasma
0	2.56	36.6	36.6	none
6	2.56	18.3	36.6	none
24	5.12	18.3	36.6	none

The MICs of conjugates were evaluated following incubation with human plasma to investigate the influence of human plasma proteases on the antibacterial activity of the TN6 peptide and conjugates. Samples were treated with *S. aureus* 25923 after sampling at 0-, 6-, and 24-hour periods, as described in the method.

Only plasma was used as a negative control, and it did not demonstrate any antibacterial activity. The pep-PEG-pep designs with the best MICs was chosen for the biological protease assay. After one day, the antibacterial activity of peptides decreased. In comparison between pepC-PEG-pepC and Cpep-PEG-Cpep conjugates, MIC was constant constant during the whole period for pepC-PEG-pepC, but Cpep-PEG-Cpep's MIC declined between 0–6 h time period (Table 4.3).

4.3.6 SEM and TEM Results

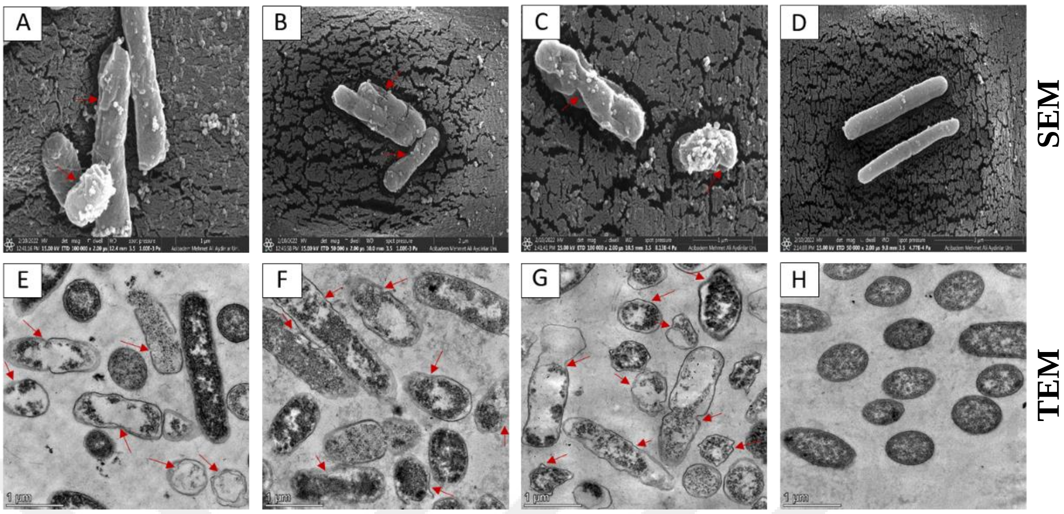

Figure 4.14 Imaging of the effect of peptides and conjugates on *E. coli* by SEM and TEM. (A, E) Cpep-PEG-Cpep, (B, F) pepC-PEG-pepC (B–F), (C, G) TN6 peptide and (D–H) *E. coli* control.

The samples shown in Figure 4.14 were treated with *E. coli* 25922 and then cellular damage was observed by SEM. Control cells without any treatment had smooth surfaces (D), but conjugate/peptide-treated cells had morphological alterations (A-C). The sections highlighted with red arrows show the changes in membrane. In bacterial membranes, Cpep-PEG-Cpep (A) and PepC-PEG-PepC (B) conjugates showed similar damage motifs.

TEM was used to investigate intracellular alterations in E. coli and differentiations of the cell wall after peptide and conjugate treatment. E. coli displayed homogenous intracellular composition and fully bacterial membrane (H). On the other hand, after peptide and conjugate treatment, caused considerable cell wall and membrane breakdown, cell content leakage, and visible clear regions in cytoplasm (E-G). Furthermore, E.coli cytoplasm became heterogeneous. The identical cellular damage motifs were seen between conjugates, Cpep-PEG-Cpep (E) and pepC-PEG-pepC (F).

5. DISCUSSION

For millions of years, various organisms have used AMPs for the self-defense (123). AMPs have become promising next-generation antibiotics because of their high antimicrobial effect, non-inducing AMR property, and broad-spectrum. The number of synthetic AMPs designed to mimic nature has increased in recent years. For instance, new AMPs produced through the creation of synthetic derivatives of cathelicidins have shown much higher antimicrobial activity than cathelicidin itself (124). However, only a small number of AMPs have received FDA approval because of their high toxicity, short plasma half-life, low stability, and poor solubility (125).

In this study, followed a PEGylation strategy to minimize the possible side effects of AMPs. For this purpose, six different novel PEG-AMP conjugates were developed to understand the effect of parameters such as the conjugation site of the PEG polymer, peptide orientation and the effect of the number of bound AMPs. TN6 peptide, a synthetic derivative of cathelicidin, was used in the developed conjugates because of its high antimicrobial activity. TN6 peptides were linked to the PEG polymer through their N- or C- termini via a terminal cysteine residue. The antimicrobial activity, protease activity, toxicity, and stability of all conjugates were systematically evaluated *in vitro*.

Since the PEG polymer is a very hydrophilic molecule, it can reduce the hydrophobic effects of the molecules to which it can be attach as a conjugate form. As seen in the HPLC results (Figure 4.1), the modified peptide peaks, which approximately observe at 45% ACN, decrease to 2,1–2,8% ACN when a single peptide is bound with one PEG molecule (PEG-pep design) and become extremely hydrophilic.

When two peptide molecules were linked in a "Y" shape from a single point with one end of the PEG molecule (PEG-(pep)$_2$ conjugates), the ratio of ACN decreased to 3,5–4,2%. Compared to PEG-pep conjugates (2,1–2,8% ACN), the reason why the hydrophilic properties do not change much despite the binding of two peptide molecules may be that in both designs the PEG polymer is closed at only one end and remains free at the other end.

pep-PEG-pep conjugates' peaks (67–70% ACN) are compared with PEG-$(pep)_2$, and the hydrophilicity of pep-PEG-pep conjugates is much lower than the PEG-$(pep)_2$ designs, although there is an equal amount of peptide. This decrease can be related to the PEG polymer in the pep-PEG-pep design staying in the middle of the peptide molecules, hiding inside its structure, and no free PEG ends are left.

It is understood from the LC/MSMS result given in Figure 4.2 that the peptide was synthesized correctly in the analyzes performed. The accurate synthesis of polymer-peptide conjugates is clearly seen in the results of FT-IR (Figure 4.3–4.6) and proton NMR (Figure 4.7–4.10).

We investigated the potential of our conjugates to become candidates for next-generation broad-spectrum antibiotics by testing PEG-AMP conjugates against different types of microorganisms (Table 4.2). The PEG polymers used were non-toxic, highly soluble molecules(126) and did not show antimicrobial activity (data not shown). The naked TN6 peptide exhibited the highest antimicrobial activity compared with the conjugates. One may speculate that an AMP attached to the PEG may show reduced activity because of the steric hindrance created by the surrounding PEG branches. Other studies observed that the antimicrobial activity of natural (127) or synthetic (128) AMPs with α-helical structure decreased after PEGylation. The reduction in antimicrobial activity can be more drastic when the active end of the AMP is masked. To understand this phenomenon, AMPs were attached from either end to the PEG polymer and evaluated. The results helped us understand which side of the peptide is more active depending on its orientation within the whole structure. Interestingly, the TN6 peptide conjugated via its N-terminus in the pep-PEG-pep design has shown the highest inhibitory effect. This would normally be regarded as the C-terminus of the TN6 peptide being required to be unattached to a structure to exhibit its activity. However, in the PEG-pep and PEG-$(pep)_2$ conjugate designs, peptide conjugation via the C-terminus exhibited superior antimicrobial activity for most of the tested microorganisms. Therefore, no generalization can be made regarding the active terminus of the AMPs in AMP-containing conjugates. This can be explained by the major difference in the conjugate designs. For the pep-PEG-pep conjugate structure, there is less possibility of the polymer being able to sterically hinder the free ends of the peptide. In this architecture, where the peptides are attached to the polymer from its different sides, the peptide is given more flexibility during its entry into the bacteria. Meanwhile, when the PEG polymer and the two peptides are attached via one branched, trifunctional linker as in the PEG-$(pep)_2$ design, antimicrobial activity is reduced. This may be due to the steric hindrance caused by the free PEG polymer on one side of the peptide and the possibility of two peptides suppressing each other's activity through non-covalent interactions. We have observed similar peptide peptides in molecular dynamics studies; that is when peptides aggregate or stay close to each other, the activity of the molecules is always reduced whereas when they are free to approach the membrane, they exert better antimicrobial activity (data not shown).

The cytotoxicity of the conjugates on mammalian cells were determined (Figure 4.11), and their MIC values were compared. The cytotoxicity of TN6 peptide was significantly higher than those of most conjugates in 3T3 and HaCaT cell lines. This indicates that the polymer–peptide conjugates reduced cytotoxicity towards the naked peptide. This may be because the hydrophilic PEG polymer forms a stable structure by preventing the aggregation of its peptide, and the polymer prevents non-specific cell and protein binding by surrounding the peptide (129,130).

When the IC50 values of the conjugates tested in the HaCaT and 3T3 cell lines were compared, all conjugates except PEG-$(pepC)_2$ showed significantly lower cytotoxicity in the HaCaT cell line. Interestingly, the PEG-$(pepC)_2$ conjugate showed the highest cytotoxicity in the HaCaT cell line but the lowest cytotoxicity in the 3T3 cell line. Therefore, only the PEG-$(pepC)_2$ conjugate exerts cytotoxicity in the HaCaT cell line based on the MIC values of conjugates. In addition, conjugates with the PEG-pep design did not exceed the IC50 in all concentrations studied. In the 3T3 cell line, the IC50 value for the Cpep-PEG-Cpep conjugate had a non-cytotoxic range at all MIC values. MIC values of the PEG-Cpep, PEG-pepC and pepC-PEG-pepC conjugates did not exceed the IC50 cytotoxicity value in all tested bacteria except *P. aeruginosa*. The PEG-(pepC)$_2$ conjugate did not exhibit cytotoxicity for the MIC values of all bacteria except *E. coli* and *P. aeruginosa*. Meanwhile, all MIC values tested in the PEG-(Cpep)$_2$ conjugate were toxic to the 3T3 cell line.

Keratinocytes and dermal fibroblasts represent the main cell type of the epidermis and dermis, respectively. The HaCaT (keratinocyte) cell line is found in all epidermis layers, while the 3T3 (fibroblast) cell line is found in the dermis (131,132). In future *in vivo* experiments, conjugates are not expected to encounter fibroblasts at desired doses (i.e., concentrations between MIC and IC50 cytotoxicity values) as in *in vitro* experiments. Therefore, most of the conjugate molecules will first reach the keratinocytes and will act in this region in the case of topical application, such as ointments. Thus, the toxic effects of the conjugates, if any, are expected to be lower for fibroblasts than the associated values obtained in *in vitro* experiments.

To evaluate the *in vitro* hemolytic effect of the peptide/conjugate, the percentage of concentration-dependent hemolysis was determined by treating compounds with human erythrocytes at different time intervals (Figure 4.12). The TN6 peptide exhibited the highest hemolytic activity at all time intervals. After 30 min of incubation, all doses tested for the TN6 peptide were shown as hemotoxic. The hemolytic activity of the peptide/conjugate increased at 60 min of treatment compared to 30 min. However, this increase made naked TN6 peptide toxic even at 1 μg/mL. Introducing the PEG polymer in the structure significantly reduced the hemolytic effect.

Bacteremia is a clinical condition characterized by the presence of bacteria in the bloodstream (133). When *S. aureus* was added to the 60 min hemolytic activity test setup, a significant decline was observed in the hemolytic activities of all conjugates (Figure 4.13). The PEG-(pepC)$_2$ conjugate (HC50: 49.60 μg/mL) had the lowest hemolytic activity at 60 min with bacteria. However, the naked TN6 peptide continued to show a hemotoxic effect even with addition of bacteria. We speculate that with the addition of bacteria, the peptide/conjugate preferentially targets the bacterial membrane rather than the erythrocyte membrane, thereby diminishing hemolytic activity. Likewise, the addition of bacteria resulted in a 15-fold decrease in the hemolytic activity of the pepC-PEG-pepC conjugate at 60 min. Therefore, the conjugates might be effective antibiotic candidates in future clinical cases such as bacteremia or sepsis.

After treatment with plasma proteases, the MIC values of the peptide/conjugate were investigated at different time points (Table 4.3). As expected, the MIC value for the TN6 peptide increased. The value for the Cpep-PEG-Cpep conjugate decreased, while that for the pepC-PEG-pepC conjugate remained constant. The reason why the antimicrobial activity of the Cpep-PEG-Cpep conjugate increases over time might be that the proteases damage the C-TN6 peptide attached to this conjugate, causing its fragmentation. Accordingly, the new peptide sequence formed with the remaining amino acids after cleavage still has a certain length, amphiphilic characteristics, and a positive charge. It might have increased its antimicrobial activity because of these properties. The results show that the resistance of the peptide to plasma proteases clearly increases during the PEGylation process.

Likewise, the TN6 peptide, a cathelicidin-like AMP, uses pattern similar to that of cathelicidins in killing microorganisms. Positively charged peptide/conjugate interacts with the negatively charged cell membranes of microorganisms to form transmembrane pores that directly kill the microorganisms (134). Peptide/conjugate also forms a hydrophilic channel between the charged groups, allowing water molecules and other hydrophilic molecules to move (124). As clearly seen in the SEM/TEM results, the cell membrane has become rough and the cell cytoplasm heterogeneous because of the transmembrane pores formed by the peptides/conjugate. In addition, intracellular compartments were observed to leak out of the membrane (Figure 4.14).

6. CONCLUSION

In conclusion, the constructs developed in this study successfully demonstrated *in vitro* antimicrobial activity against six different microorganism types. These properties and their low adverse effects highlight PEG-AMP conjugates as potential next-generation broad-spectrum antibiotics. Moreover, they can be considered promising candidates for addressing the lack of suitable drugs against various pathogen-resistant microorganisms.

7. REFERENCES

1. Global action plan on antimicrobial resistance [Internet]. [a.yer 09 Nisan 2023]. Erişim adresi: https://fctc.who.int/publications/i/item/global-action-plan-on-antimicrobial-resistance
2. Singh KS, Anand S, Dholpuria S, Sharma JK, Blankenfeldt W, Shouche Y. Antimicrobial resistance dynamics and the one-health strategy: a review. Environ Chem Lett. 01 Ağustos 2021;19(4):2995-3007.
3. Ventola CL. The Antibiotic Resistance Crisis: Part 1: Causes and Threats. Pharm Ther. Nisan 2015;40(4):277.
4. Mittal AK, Bhardwaj R, Mishra P, Rajput SK. Antimicrobials Misuse/Overuse: Adverse Effect, Mechanism, Challenges and Strategies to Combat Resistance. Open Biotechnol J [Internet]. 08 Eylül 2020 [a.yer 09 Nisan 2023];14(1). Erişim adresi: https://openbiotechnologyjournal.com/VOLUME/14/PAGE/107/
5. Critically important antimicrobials for human medicine : 6th revision [Internet]. [a.yer 09 Nisan 2023]. Erişim adresi: https://www.who.int/publications-detail-redirect/9789241515528
6. Trotter AJ, Aydin A, Strinden MJ, O'Grady J. Recent and emerging technologies for the rapid diagnosis of infection and antimicrobial resistance. Curr Opin Microbiol. Ekim 2019;51:39-45.
7. Irfan M, Almotiri A, AlZeyadi ZA. Antimicrobial Resistance and Its Drivers—A Review. Antibiotics. Ekim 2022;11(10):1362.
8. Demeke CA, Adinew GM, Abebe TB, Gelaye AT, Gemeda SG, Yimenu DK. Comparative analysis of the effectiveness of narrow-spectrum versus broad-spectrum antibiotics for the treatment of childhood pneumonia. SAGE Open Med. 09 Eylül 2021;9:20503121211044380.
9. De Pascale G, Wright GD. Antibiotic Resistance by Enzyme Inactivation: From Mechanisms to Solutions. ChemBioChem. 2010;11(10):1325-34.
10. Wright GD. Bacterial resistance to antibiotics: Enzymatic degradation and modification. Adv Drug Deliv Rev. 29 Temmuz 2005;57(10):1451-70.
11. Lambert PA. Bacterial resistance to antibiotics: Modified target sites. Adv Drug Deliv Rev. 29 Temmuz 2005;57(10):1471-85.
12. Schaenzer AJ, Wright GD. Antibiotic Resistance by Enzymatic Modification of Antibiotic Targets. Trends Mol Med. 01 Ağustos 2020;26(8):768-82.
13. Then RL. Mechanisms of Resistance to Trimethoprim, the Sulfonamides, and Trimethoprim-Sulfamethoxazole. Rev Infect Dis. 01 Mart 1982;4(2):261-9.
14. Fernández L, Hancock REW. Adaptive and Mutational Resistance: Role of Porins and Efflux Pumps in Drug Resistance. Clin Microbiol Rev. Ekim 2012;25(4):661-81.
15. Webber MA, Piddock LJV. The importance of efflux pumps in bacterial antibiotic resistance. J Antimicrob Chemother. 01 Ocak 2003;51(1):9-11.
16. Wilson DN, Hauryliuk V, Atkinson GC, O'Neill AJ. Target protection as a key antibiotic resistance mechanism. Nat Rev Microbiol. Kasım 2020;18(11):637-48.
17. Darby EM, Trampari E, Siasat P, Gaya MS, Alav I, Webber MA, vd. Molecular mechanisms of antibiotic resistance revisited. Nat Rev Microbiol. 21 Kasım 2022;1-16.
18. Cummins EA, Snaith AE, McNally A, Hall RJ. The role of potentiating mutations in the evolution of pandemic Escherichia coli clones. Eur J Clin Microbiol Infect Dis [Internet]. 17 Kasım 2021 [a.yer 12 Nisan 2023]; Erişim adresi: https://doi.org/10.1007/s10096-021-04359-3
19. Gomez-Simmonds A, Uhlemann AC. Clinical Implications of Genomic Adaptation and Evolution of Carbapenem-Resistant Klebsiella pneumoniae. J Infect Dis. 15 Şubat 2017;215(suppl_1):S18-27.
20. Ramsay RR, Tipton KF. Assessment of Enzyme Inhibition: A Review with Examples from the Development of Monoamine Oxidase and Cholinesterase Inhibitory Drugs. Molecules. Temmuz 2017;22(7):1192.
21. Simões M, Bennett RN, Rosa EAS. Understanding antimicrobial activities of phytochemicals against multidrug resistant bacteria and biofilms. Nat Prod Rep. 27 Mayıs 2009;26(6):746-57.
22. Abreu AC, McBain AJ, Simões M. Plants as sources of new antimicrobials and resistance-modifying agents. Nat Prod Rep. 07 Ağustos 2012;29(9):1007-21.
23. Theuretzbacher U, Outterson K, Engel A, Karlén A. The global preclinical antibacterial pipeline. Nat Rev Microbiol. Mayıs 2020;18(5):275-85.

24. Ryan MD, Parkes AL, Corbett D, Dickie AP, Southey M, Andersen OA, vd. Discovery of Novel UDP-N-Acetylglucosamine Acyltransferase (LpxA) Inhibitors with Activity against Pseudomonas aeruginosa. J Med Chem. 14 Ekim 2021;64(19):14377-425.
25. Molchanova N, Hansen PR, Franzyk H. Advances in Development of Antimicrobial Peptidomimetics as Potential Drugs. Molecules. Eylül 2017;22(9):1430.
26. Rima M, Rima M, Fajloun Z, Sabatier JM, Bechinger B, Naas T. Antimicrobial Peptides: A Potent Alternative to Antibiotics. Antibiotics. Eylül 2021;10(9):1095.
27. Brogden KA. Antimicrobial peptides: pore formers or metabolic inhibitors in bacteria? Nat Rev Microbiol. Mart 2005;3(3):238-50.
28. Nguyen LT, Haney EF, Vogel HJ. The expanding scope of antimicrobial peptide structures and their modes of action. Trends Biotechnol. 01 Eylül 2011;29(9):464-72.
29. Wright GD. Opportunities for natural products in 21st century antibiotic discovery. Nat Prod Rep. 01 Temmuz 2017;34(7):694-701.
30. Stach J, Good L. Synthetic RNA Silencing in Bacteria – Antimicrobial Discovery and Resistance Breaking. Front Microbiol [İnternet]. 2011 [a.yer 15 Nisan 2023];2. Erişim adresi: https://www.frontiersin.org/articles/10.3389/fmicb.2011.00185
31. Duan C, Cao H, Zhang LH, Xu Z. Harnessing the CRISPR-Cas Systems to Combat Antimicrobial Resistance. Front Microbiol [İnternet]. 2021 [a.yer 15 Nisan 2023];12. Erişim adresi: https://www.frontiersin.org/articles/10.3389/fmicb.2021.716064
32. Gholizadeh P, Köse Ş, Dao S, Ganbarov K, Tanomand A, Dal T, vd. How CRISPR-Cas System Could Be Used to Combat Antimicrobial Resistance. Infect Drug Resist. 15 Nisan 2020;13:1111-21.
33. Yang SK, Tan NP, Chong CW, Abushelaibi A, Lim SHE, Lai KS. The Missing Piece: Recent Approaches Investigating the Antimicrobial Mode of Action of Essential Oils. Evol Bioinforma. 01 Ocak 2021;17:1176934320938391.
34. Gill AO, Holley RA. Disruption of Escherichia coli, Listeria monocytogenes and Lactobacillus sakei cellular membranes by plant oil aromatics. Int J Food Microbiol. 15 Nisan 2006;108(1):1-9.
35. Yap PSX, Yiap BC, Ping HC, Lim SHE. Essential Oils, A New Horizon in Combating Bacterial Antibiotic Resistance. Open Microbiol J. 07 Şubat 2014;8:6-14.
36. Iseppi R, Mariani M, Condò C, Sabia C, Messi P. Essential Oils: A Natural Weapon against Antibiotic-Resistant Bacteria Responsible for Nosocomial Infections. Antibiotics. Nisan 2021;10(4):417.
37. McAuliffe O, Ross RP, Hill C. Lantibiotics: structure, biosynthesis and mode of action. FEMS Microbiol Rev. 01 Mayıs 2001;25(3):285-308.
38. Cotter PD, Ross RP, Hill C. Bacteriocins — a viable alternative to antibiotics? Nat Rev Microbiol. Şubat 2013;11(2):95-105.
39. Otvos L Jr. Antibacterial peptides isolated from insects. J Pept Sci. 2000;6(10):497-511.
40. Sahoo A, Swain SS, Behera A, Sahoo G, Mahapatra PK, Panda SK. Antimicrobial Peptides Derived From Insects Offer a Novel Therapeutic Option to Combat Biofilm: A Review. Front Microbiol [İnternet]. 2021 [a.yer 16 Nisan 2023];12. Erişim adresi: https://www.frontiersin.org/articles/10.3389/fmicb.2021.661195
41. Lee JS, Chung MJ, Seo JG. In Vitro Evaluation of Antimicrobial Activity of Lactic Acid Bacteria against Clostridium difficile. Toxicol Res. 01 Haziran 2013;29(2):99-106.
42. Palma E, Tilocca B, Roncada P. Antimicrobial Resistance in Veterinary Medicine: An Overview. Int J Mol Sci. Ocak 2020;21(6):1914.
43. Aponte M, Murru N, Shoukat M. Therapeutic, Prophylactic, and Functional Use of Probiotics: A Current Perspective. Front Microbiol [İnternet]. 2020 [a.yer 16 Nisan 2023];11. Erişim adresi: https://www.frontiersin.org/articles/10.3389/fmicb.2020.562048
44. Zurawski DV, McLendon MK. Monoclonal Antibodies as an Antibacterial Approach Against Bacterial Pathogens. Antibiotics. Nisan 2020;9(4):155.
45. Motley MP, Banerjee K, Fries BC. Monoclonal Antibody-Based Therapies for Bacterial Infections. Curr Opin Infect Dis. Haziran 2019;32(3):210-6.
46. Ofir G, Sorek R. Contemporary Phage Biology: From Classic Models to New Insights. Cell. 08 Mart 2018;172(6):1260-70.
47. Jamal M, Ahmad W, Andleeb S, Jalil F, Imran M, Nawaz MA, vd. Bacterial biofilm and associated infections. J Chin Med Assoc. 01 Ocak 2018;81(1):7-11.
48. Wille J, Coenye T. Biofilm dispersion: The key to biofilm eradication or opening Pandora’s box? Biofilm. 01 Aralık 2020;2:100027.

49. Windels EM, Michiels JE, Fauvart M, Wenseleers T, Van den Bergh B, Michiels J. Bacterial persistence promotes the evolution of antibiotic resistance by increasing survival and mutation rates. ISME J. Mayıs 2019;13(5):1239-51.
50. Salcedo-Sora JE, Kell DB. A Quantitative Survey of Bacterial Persistence in the Presence of Antibiotics: Towards Antipersister Antimicrobial Discovery. Antibiotics. Ağustos 2020;9(8):508.
51. Solano C, Echeverz M, Lasa I. Biofilm dispersion and quorum sensing. Curr Opin Microbiol. 01 Nisan 2014;18:96-104.
52. Rémy B, Mion S, Plener L, Elias M, Chabrière E, Daudé D. Interference in Bacterial Quorum Sensing: A Biopharmaceutical Perspective. Front Pharmacol [İnternet]. 2018 [a.yer 18 Nisan 2023];9. Erişim adresi: https://www.frontiersin.org/articles/10.3389/fphar.2018.00203
53. Zhao X, Yu Z, Ding T. Quorum-Sensing Regulation of Antimicrobial Resistance in Bacteria. Microorganisms. Mart 2020;8(3):425.
54. Gao J, Karp JM, Langer R, Joshi N. The Future of Drug Delivery. Chem Mater. 24 Ocak 2023;35(2):359-63.
55. Pham TN, Loupias P, Dassonville-Klimpt A, Sonnet P. Drug delivery systems designed to overcome antimicrobial resistance. Med Res Rev. 2019;39(6):2343-96.
56. Möllmann U, Heinisch L, Bauernfeind A, Köhler T, Ankel-Fuchs D. Siderophores as drug delivery agents: application of the “Trojan Horse” strategy. BioMetals. 01 Ağustos 2009;22(4):615-24.
57. Qiu Y, Xu D, Sui G, Wang D, Wu M, Han L, vd. Gentamicin decorated phosphatidylcholine-chitosan nanoparticles against biofilms and intracellular bacteria. Int J Biol Macromol. 01 Ağustos 2020;156:640-7.
58. Spirescu VA, Chircov C, Grumezescu AM, Andronescu E. Polymeric Nanoparticles for Antimicrobial Therapies: An up-to-date Overview. Polymers. Ocak 2021;13(5):724.
59. Li M, Du C, Guo N, Teng Y, Meng X, Sun H, vd. Composition design and medical application of liposomes. Eur J Med Chem. 15 Şubat 2019;164:640-53.
60. Ferreira M, Ogren M, Dias JNR, Silva M, Gil S, Tavares L, vd. Liposomes as Antibiotic Delivery Systems: A Promising Nanotechnological Strategy against Antimicrobial Resistance. Molecules. Ocak 2021;26(7):2047.
61. Augustin M, Goepel L, Jacobi A, Bosse B, Mueller S, Hopp M. Efficacy and tolerability of liposomal polyvinylpyrrolidone-iodine hydrogel for the localized treatment of chronic infective, inflammatory, dermatoses: an uncontrolled pilot study. Clin Cosmet Investig Dermatol. 31 Aralık 2017;10:373-84.
62. Alipour M, Halwani M, Omri A, Suntres ZE. Antimicrobial effectiveness of liposomal polymyxin B against resistant Gram-negative bacterial strains. Int J Pharm. 01 Mayıs 2008;355(1):293-8.
63. Deng R, Zhou C, Li D, Cai H, Sukumaran S, Carrasco-Triguero M, vd. Preclinical and translational pharmacokinetics of a novel THIOMAB™ antibody-antibiotic conjugate against Staphylococcus aureus. mAbs. 18 Ağustos 2019;11(6):1162-74.
64. Brun P, Bernabè G, Marchiori C, Scarpa M, Zuin M, Cavazzana R, vd. Antibacterial efficacy and mechanisms of action of low power atmospheric pressure cold plasma: membrane permeability, biofilm penetration and antimicrobial sensitization. J Appl Microbiol. 01 Ağustos 2018;125(2):398-408.
65. Bourke P, Ziuzina D, Han L, Cullen PJ, Gilmore BF. Microbiological interactions with cold plasma. J Appl Microbiol. 01 Ağustos 2017;123(2):308-24.
66. Mai-Prochnow A, Murphy AB, McLean KM, Kong MG, Ostrikov K (Ken). Atmospheric pressure plasmas: Infection control and bacterial responses. Int J Antimicrob Agents. 01 Haziran 2014;43(6):508-17.
67. Heinlin J, Isbary G, Stolz W, Zeman F, Landthaler M, Morfill G, vd. A randomized two-sided placebo-controlled study on the efficacy and safety of atmospheric non-thermal argon plasma for pruritus. J Eur Acad Dermatol Venereol. 2013;27(3):324-31.
68. Maisch T, Shimizu T, Li YF, Heinlin J, Karrer S, Morfill G, vd. Decolonisation of MRSA, S. aureus and E. coli by Cold-Atmospheric Plasma Using a Porcine Skin Model In Vitro. PLOS ONE. 27 Nisan 2012;7(4):e34610.
69. Zeina B, Greenman J, Purcell WM, Das B. Killing of cutaneous microbial species by photodynamic therapy. Br J Dermatol. 01 Şubat 2001;144(2):274-8.
70. Oyim J, Omolo CA, Amuhaya EK. Photodynamic Antimicrobial Chemotherapy: Advancements in Porphyrin-Based Photosensitize Development. Front Chem. 2021;9:635344.
71. Serpe L, Giuntini F. Sonodynamic antimicrobial chemotherapy: First steps towards a sound approach for microbe inactivation. J Photochem Photobiol B. 01 Eylül 2015;150:44-9.

72. Harris F, Dennison SR, Phoenix DA. Using sound for microbial eradication – light at the end of the tunnel? FEMS Microbiol Lett. 01 Temmuz 2014;356(1):20-2.
73. Erriu M, Blus C, Szmukler-Moncler S, Buogo S, Levi R, Barbato G, vd. Microbial biofilm modulation by ultrasound: current concepts and controversies. Ultrason Sonochem. Ocak 2014;21(1):15-22.
74. Rosenthal I, Sostaric JZ, Riesz P. Sonodynamic therapy—a review of the synergistic effects of drugs and ultrasound. Ultrason Sonochem. 01 Eylül 2004;11(6):349-63.
75. Nayab S, Aslam MA, Rahman S ur, Sindhu Z ud D, Sajid S, Zafar N, vd. A Review of Antimicrobial Peptides: Its Function, Mode of Action and Therapeutic Potential. Int J Pept Res Ther. 07 Ocak 2022;28(1):46.
76. Zhang L juan, Gallo RL. Antimicrobial peptides. Curr Biol. 11 Ocak 2016;26(1):R14-9.
77. Erdem Büyükkiraz M, Kesmen Z. Antimicrobial peptides (AMPs): A promising class of antimicrobial compounds. J Appl Microbiol. 2022;132(3):1573-96.
78. Hancock REW, Sahl HG. Antimicrobial and host-defense peptides as new anti-infective therapeutic strategies. Nat Biotechnol. Aralık 2006;24(12):1551-7.
79. Lei J, Sun L, Huang S, Zhu C, Li P, He J, vd. The antimicrobial peptides and their potential clinical applications. Am J Transl Res. 2019;11(7):3919-31.
80. Kumar P, Kizhakkedathu JN, Straus SK. Antimicrobial Peptides: Diversity, Mechanism of Action and Strategies to Improve the Activity and Biocompatibility In Vivo. Biomolecules. Mart 2018;8(1):4.
81. Huan Y, Kong Q, Mou H, Yi H. Antimicrobial Peptides: Classification, Design, Application and Research Progress in Multiple Fields. Front Microbiol [İnternet]. 2020 [a.yer 24 Ocak 2023];11. Erişim adresi: https://www.frontiersin.org/articles/10.3389/fmicb.2020.582779
82. Wimley WC. Describing the Mechanism of Antimicrobial Peptide Action with the Interfacial Activity Model. ACS Chem Biol. 15 Ekim 2010;5(10):905-17.
83. Goyal R, Mattoo A. Plant Antimicrobial Peptides. İçinde 2016. s. 111-36.
84. Shai Y, Oren Z. From "carpet" mechanism to de-novo designed diastereomeric cell-selective antimicrobial peptides. Peptides. 01 Ekim 2001;22(10):1629-41.
85. Le CF, Fang CM, Sekaran SD. Intracellular Targeting Mechanisms by Antimicrobial Peptides. Antimicrob Agents Chemother. Nisan 2017;61(4):e02340-16.
86. Moulay G, Leborgne C, Mason AJ, Aisenbrey C, Kichler A, Bechinger B. Histidine-rich designer peptides of the LAH4 family promote cell delivery of a multitude of cargo. J Pept Sci Off Publ Eur Pept Soc. Nisan 2017;23(4):320-8.
87. Chongsiriwatana NP, Lin JS, Kapoor R, Wetzler M, Rea JAC, Didwania MK, vd. Intracellular biomass flocculation as a key mechanism of rapid bacterial killing by cationic, amphipathic antimicrobial peptides and peptoids. Sci Rep. 01 Aralık 2017;7(1):16718.
88. Liu C, Qi J, Shan B, Gao R, Gao F, Xie H, vd. Pretreatment with cathelicidin-BF ameliorates Pseudomonas aeruginosa pneumonia in mice by enhancing NETosis and the autophagy of recruited neutrophils and macrophages. Int Immunopharmacol. 01 Aralık 2018;65:382-91.
89. de la Fuente-Núñez C, Korolik V, Bains M, Nguyen U, Breidenstein EBM, Horsman S, vd. Inhibition of bacterial biofilm formation and swarming motility by a small synthetic cationic peptide. Antimicrob Agents Chemother. Mayıs 2012;56(5):2696-704.
90. Overhage J, Campisano A, Bains M, Torfs ECW, Rehm BHA, Hancock REW. Human host defense peptide LL-37 prevents bacterial biofilm formation. Infect Immun. Eylül 2008;76(9):4176-82.
91. Sawasaki T, Ogasawara T, Morishita R, Endo Y. A cell-free protein synthesis system for high-throughput proteomics. Proc Natl Acad Sci. 12 Kasım 2002;99(23):14652-7.
92. Wu CL, Chih YH, Hsieh HY, Peng KL, Lee YZ, Yip BS, vd. High Level Expression and Purification of Cecropin-like Antimicrobial Peptides in Escherichia coli. Biomedicines. Haziran 2022;10(6):1351.
93. Cheng KT, Wu CL, Yip BS, Yu HY, Cheng HT, Chih YH, vd. High Level Expression and Purification of the Clinically Active Antimicrobial Peptide P-113 in Escherichia coli. Molecules. Nisan 2018;23(4):800.
94. Li Y. Recombinant production of antimicrobial peptides in Escherichia coli: A review. Protein Expr Purif. 01 Aralık 2011;80(2):260-7.
95. Tippelt A, Nett M. Saccharomyces cerevisiae as host for the recombinant production of polyketides and nonribosomal peptides. Microb Cell Factories. 19 Ağustos 2021;20(1):161.

96. Cao J, de la Fuente-Nunez C, Ou RW, Torres MDT, Pande SG, Sinskey AJ, vd. Yeast-Based Synthetic Biology Platform for Antimicrobial Peptide Production. ACS Synth Biol. 16 Mart 2018;7(3):896-902.
97. Javadpour MM, Juban MM, Lo WC, Bishop SM, Alberty JB, Cowell SM, vd. De novo antimicrobial peptides with low mammalian cell toxicity. J Med Chem. 02 Ağustos 1996;39(16):3107-13.
98. Dondapati SK, Stech M, Zemella A, Kubick S. Cell-Free Protein Synthesis: A Promising Option for Future Drug Development. BioDrugs. 01 Haziran 2020;34(3):327-48.
99. Zhang L, Lin X, Wang T, Guo W, Lu Y. Development and comparison of cell-free protein synthesis systems derived from typical bacterial chassis. Bioresour Bioprocess. 06 Temmuz 2021;8(1):58.
100. Gregorio NE, Levine MZ, Oza JP. A User’s Guide to Cell-Free Protein Synthesis. Methods Protoc. Mart 2019;2(1):24.
101. Cell-free protein synthesis | Sigma-Aldrich [Internet]. [a.yer 23 Nisan 2023]. Erişim adresi: https://www.sigmaaldrich.com/TR/en/search/cell-free-protein-synthesis?focus=products&page=1&perpage=30&sort=relevance&term=cell-free+protein+synthesis&type=product_name
102. Merrifield RB. Solid Phase Peptide Synthesis. I. The Synthesis of a Tetrapeptide. J Am Chem Soc. 01 Temmuz 1963;85(14):2149-54.
103. Hansen PR, Oddo A. Fmoc Solid-Phase Peptide Synthesis. Içinde: Houen G, editör. Peptide Antibodies [Internet]. New York, NY: Springer New York; 2015 [a.yer 24 Nisan 2023]. s. 33-50. (Methods in Molecular Biology; c. 1348). Erişim adresi: https://link.springer.com/10.1007/978-1-4939-2999-3_5
104. Behrendt R, White P, Offer J. Advances in Fmoc solid-phase peptide synthesis. J Pept Sci. 2016;22(1):4-27.
105. Rezende SB, Oshiro KGN, Júnior NGO, Franco OL, Cardoso MH. Advances on chemically modified antimicrobial peptides for generating peptide antibiotics. Chem Commun. 04 Kasım 2021;57(88):11578-90.
106. Eras A, Castillo D, Suárez M, Vispo NS, Albericio F, Rodriguez H. Chemical Conjugation in Drug Delivery Systems. Front Chem [İnternet]. 2022 [a.yer 24 Nisan 2023];10. Erişim adresi: https://www.frontiersin.org/articles/10.3389/fchem.2022.889083
107. Elzahhar P, Belal ASF, Elamrawy F, Helal NA, Nounou MI. Bioconjugation in Drug Delivery: Practical Perspectives and Future Perceptions. Içinde: Weissig V, Elbayoumi T, editörler. Pharmaceutical Nanotechnology [Internet]. New York, NY: Springer New York; 2019 [a.yer 24 Nisan 2023]. s. 125-82. (Methods in Molecular Biology; c. 2000). Erişim adresi: http://link.springer.com/10.1007/978-1-4939-9516-5_11
108. Kalia J, Raines RT. Advances in Bioconjugation. Curr Org Chem. Ocak 2010;14(2):138-47.
109. Hermanson GT. Chapter 1 - Introduction to Bioconjugation. Içinde: Hermanson GT, editör. Bioconjugate Techniques (Third Edition) [Internet]. Boston: Academic Press; 2013 [a.yer 24 Nisan 2023]. s. 1-125. Erişim adresi: https://www.sciencedirect.com/science/article/pii/B9780123822390000017
110. The covalent bioconjugate of multiwalled carbon nanotube and amino-modified linearized plasmid DNA for gene delivery - Geyik - 2014 - Biotechnology Progress - Wiley Online Library [İnternet]. [a.yer 25 Nisan 2023]. Erişim adresi: https://aiche.onlinelibrary.wiley.com/doi/10.1002/btpr.1836
111. Duncan R. The dawning era of polymer therapeutics. Nat Rev Drug Discov. Mayıs 2003;2(5):347-60.
112. Veronese FM, Mero A. The impact of PEGylation on biological therapies. BioDrugs Clin Immunother Biopharm Gene Ther. 2008;22(5):315-29.
113. Veronese FM, Harris JM. Introduction and overview of peptide and protein pegylation. Adv Drug Deliv Rev. 17 Haziran 2002;54(4):453-6.
114. Pasut G, Sergi M, Veronese FM. Anti-cancer PEG-enzymes: 30 years old, but still a current approach. Adv Drug Deliv Rev. 03 Ocak 2008;60(1):69-78.
115. Roelfsema F, Biermasz NR, Pereira AM, Romijn JM. Nanomedicines in the treatment of acromegaly: focus on pegvisomant. Int J Nanomedicine. Aralık 2006;1(4):385-98.
116. Bailon P, Palleroni A, Schaffer CA, Spence CL, Fung WJ, Porter JE, vd. Rational Design of a Potent, Long-Lasting Form of Interferon: A 40 kDa Branched Polyethylene Glycol-Conjugated Interferon α-2a for the Treatment of Hepatitis C. Bioconjug Chem. 01 Mart 2001;12(2):195-202.

117. Treatment of Acromegaly with the Growth Hormone–Receptor Antagonist Pegvisomant | NEJM [İnternet]. [a.yer 26 Nisan 2023]. Erişim adresi: https://www.nejm.org/doi/full/10.1056/NEJM200004203421604
118. Wang YS, Youngster S, Grace M, Bausch J, Bordens R, Wyss DF. Structural and biological characterization of pegylated recombinant interferon alpha-2b and its therapeutic implications. Adv Drug Deliv Rev. 17 Haziran 2002;54(4):547-70.
119. Stawikowski M, Fields GB. Introduction to Peptide Synthesis. Curr Protoc Protein Sci Editor Board John E Coligan Al. Şubat 2002;CHAPTER:Unit-18.1.
120. Eren T, Som A, Rennie JR, Nelson CF, Urgina Y, Nüsslein K, vd. Antibacterial and Hemolytic Activities of Quaternary Pyridinium Functionalized Polynorbornenes. Macromol Chem Phys. 05 Mart 2008;209(5):516-24.
121. Lu J, Xu H, Xia J, Ma J, Xu J, Li Y, vd. D- and Unnatural Amino Acid Substituted Antimicrobial Peptides With Improved Proteolytic Resistance and Their Proteolytic Degradation Characteristics. Front Microbiol [İnternet]. 2020 [a.yer 20 Ocak 2023];11. Erişim adresi: https://www.frontiersin.org/articles/10.3389/fmicb.2020.563030
122. Hartmann M, Berditsch M, Hawecker J, Ardakani MF, Gerthsen D, Ulrich AS. Damage of the bacterial cell envelope by antimicrobial peptides gramicidin S and PGLa as revealed by transmission and scanning electron microscopy. Antimicrob Agents Chemother. Ağustos 2010;54(8):3132-42.
123. Zasloff M. Antimicrobial peptides of multicellular organisms. Nature. Ocak 2002;415(6870):389-95.
124. Unubol N, Selim Cinaroglu S, Elmas MA, Akcelik S, Ozal Ildeniz AT, Arbak S, vd. Peptide Antibiotics Developed by Mimicking Natural Antimicrobial Peptides. Clin Microbiol Open Access [Internet]. 2017 [a.yer 24 Ocak 2023];06(04). Erişim adresi: https://www.omicsonline.org/open-access/peptide-antibiotics-developed-by-mimicking-natural-antimicrobial-peptides-2327-5073-1000291.php?aid=92772
125. Mani M, Reddy D, Kumavath R, Ghosh P, Azevedo V, Barh D. Clinical Applications of Antimicrobial Peptides (AMPs): Where do we Stand Now? 26 Kasım 2019;
126. Roberts MJ, Bentley MD, Harris JM. Chemistry for peptide and protein PEGylation. Adv Drug Deliv Rev. 17 Haziran 2002;54(4):459-76.
127. Dennison SR, Reddy SM, Morton LHG, Harris F, Badiani K, Phoenix DA. PEGylation enhances the antibacterial and therapeutic potential of amphibian host defence peptides. Biochim Biophys Acta BBA - Biomembr. 01 Şubat 2022;1864(1):183806.
128. Morris CJ, Beck K, Fox MA, Ulaeto D, Clark GC, Gumbleton M. Pegylation of Antimicrobial Peptides Maintains the Active Peptide Conformation, Model Membrane Interactions, and Antimicrobial Activity while Improving Lung Tissue Biocompatibility following Airway Delivery. Antimicrob Agents Chemother. Haziran 2012;56(6):3298-308.
129. Pasut G, Veronese FM. State of the art in PEGylation: The great versatility achieved after forty years of research. J Controlled Release. 2012;161(2):461.
130. Zhao H, Yang K, Martinez A, Basu A, Chintala R, Liu HC, vd. Linear and branched bicin linkers for releasable PEGylation of macromolecules: controlled release in vivo and in vitro from mono- and multi-PEGylated proteins. Bioconjug Chem. 2006;17(2):341-51.
131. Benson HAE, Grice JE, Mohammed Y, Namjoshi S, Roberts MS. Topical and Transdermal Drug Delivery: From Simple Potions to Smart Technologies. Curr Drug Deliv. Haziran 2019;16(5):444-60.
132. Yousef H, Alhajj M, Sharma S. Anatomy, Skin (Integument), Epidermis. Içinde: StatPearls [Internet]. Treasure Island (FL): StatPearls Publishing; 2022 [a.yer 14 Şubat 2023]. Erişim adresi: http://www.ncbi.nlm.nih.gov/books/NBK470464/
133. van Hal SJ, Jensen SO, Vaska VL, Espedido BA, Paterson DL, Gosbell IB. Predictors of mortality in Staphylococcus aureus Bacteremia. Clin Microbiol Rev. Nisan 2012;25(2):362-86.
134. Amer LS, Bishop BM, van Hoek ML. Antimicrobial and antibiofilm activity of cathelicidins and short, synthetic peptides against Francisella. Biochem Biophys Res Commun. 28 Mayıs 2010;396(2):246-51.

8. APPENDIX

Appendix 1 Standard curve for peptide and conjugate concentration

Standards of peptide and conjugate concentration measurements were prepared using peptide standards included in the Pierce™ Quantitative Fluorometric Peptide Assay kit (Thermo Scientific™), and measurements were taken using the UV-vis spectrophotometer at Ex/Em 214 nm. In the standard curve representing, 8 serial dilutions were made from Standard A (1 mg/mL) and the standard was prepared and used. Concentration calculations were calculated with the formula given in eq.1. Measurements and the calibration curve is shown below.

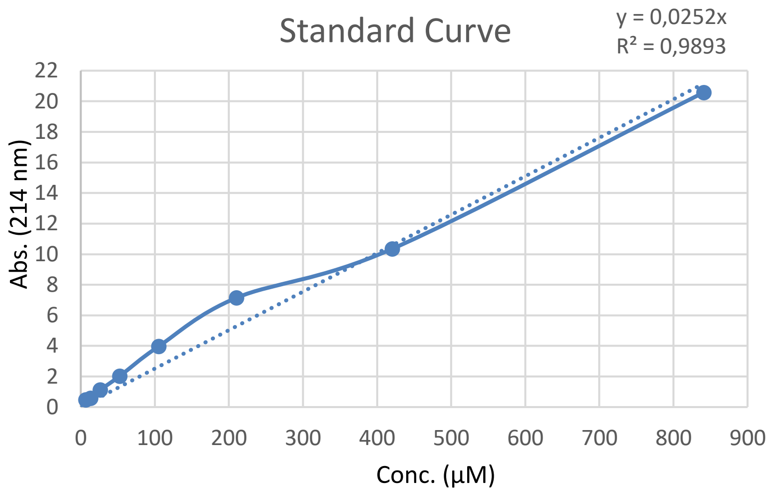

Figure 8.1 Standard curve for polymer-peptide conjugate and peptide concentration.

Appendix 2 Ethical authorization of the research

This study was approved by Acıbadem Mehmet Ali Aydınlar University Medical Research Ethics Committee (ATADEK) (Ethics Committee decision no. ATADEK 2023-2/32).

9. CURRICULUM VITAE